



Investigation of spatio-temporal variability of meteorological drought in the Luni River Basin, Rajasthan, India

Jiarul Alam¹ · Piu Saha¹ · Rajib Mitra¹ · Jayanta Das²

Received: 2 September 2022 / Accepted: 3 February 2023 / Published online: 24 February 2023
© Saudi Society for Geosciences and Springer Nature Switzerland AG 2023

Abstract

Drought is one of the most serious natural disasters that threaten human societies and environments in nearly every region of the world; therefore, evaluating drought is becoming increasingly important and helpful in eradicating the effects of climate change. This study investigates the spatiotemporal drought pattern over the Luni basin from 1959 to 2019. This research analyzed spatio-temporal drought status using the standardized precipitation index (SPI). The drought trends were analyzed using the Mann-Kendall (MK) test or modified MK test and graphical innovative trend analysis (ITA). The SPI result shows that 39 studied stations are subject to mild to severe drought. The MK/mMK trend test results detected only a monotonic trend of drought across different time ranges and locations within the study area, where the ITA trend test revealed that 43% of the recorded rain gauge stations experienced a non-monotonic negative trend, more than 23% of stations were experienced a monotonic positive trend and 10% non-monotonic positive trend. In addition, with the exception of some small patches of western and eastern parts, the Z statistic result did not reveal any significant trend. The results showed that the ITA approach is more consistent than the MK test and can detect monotonic and non-monotonic trends that the MK method cannot detect. This research provided evidence that drought trends can be studied using the ITA approach, and the results of this analysis would be very useful for identifying droughts to develop effective management plans.

Keywords Drought · Rainfall · Standardized precipitation index · Mann-Kendall · Innovative trend analysis · Luni basin

Introduction

The natural occurrences of drought cause the reduction of water availability with inadequate rainfall. Drought is a severe natural recurring hazard that develops due to

a seasonal or longer precipitation shortage and results in reducing the availability of water (Kamruzzaman et al. 2022; Alsubih et al. 2021). It is a multifaceted dangerous occurrence that impacts almost every climatic region in the world and poses a severe threat to the global population (Tran et al. 2020). The semi-arid areas are particularly vulnerable to drought due to low annual precipitation (Masroor et al. 2020) and sensitivity to climate change (Gupta et al. 2020; Mitra and Kumar Mandal 2022). However, the occurrences of drought, its magnitudes, and its cyclic nature are very hard to predict (Sirdaş and Sen 2003). Moreover, drought is the most complicated and exiguous perceived phenomenon among all kinds of natural hazards (Zhang et al. 2016). Like the other natural hazard, drought is not a sudden phenomenon (Masroor et al. 2020) rather, it is a creeping climatic phenomenon that frequently occurs with its intense impact. Several factors govern drought, one of which is rainfall is the leading factor (Mishra et al. 2021); hence, the lack of rainfall accelerates the drought (Pathak and Dodamani 2020). However, the declining total amount of rain that falls over a long time compared to the normal condition and the changing

Responsible Editor: Zhihua Zhang

✉ Jayanta Das
jayanta.daas@gmail.com

Jiarul Alam
geojia94@gmail.com

Piu Saha
piusaha.nbu@gmail.com

Rajib Mitra
rajibmitrageo@gmail.com

¹ Department of Geography and Applied Geography, University of North Bengal, PO- North Bengal University, Dist- Darjeeling 734013, India

² Department of Geography, Rampurhat College, PO- Rampurhat, Dist- Birbhum 731224, India

weather pattern with increasing temperature, solar radiation, and decreasing cloudiness and humidity are known as meteorological drought (Zhang et al. 2016).

Drought is a natural tragedy in India, where rainfall fluctuates both spatially and temporally (Patel et al. 2007). According to IMD, if rainfall is less than 75% of normal, then it is called that the area is under a drought situation (Shewale and Kumar 2005). Around two-thirds of India's land area receives very little rainfall, with uneven and unpredictable distributions (Ganguli and Reddi 2013). Additionally, In India, about 68% of the net sown land is at risk of drought, and half of this risk area is categorized as "extreme" with drought occurring almost regularly (Murthy and Sai 2010). However, the state of Rajasthan faces the highest likelihood of drought occurrence, with recurrent around 3 to 4 years in 5 years of drought (Mall et al. 2006), and from 1901 to 2002, 48 drought years were found in Rajasthan (Rathore 2004). The outcome of decreasing seasonal rainfall in east and west Rajasthan was 60 and 71%, respectively, with various degrees of severity that affected nearly a quarter of the country (Ganguli and Reddy 2014). Moreover, in 2001 Rajasthan received just 381 mm of rainfall during the monsoon period, resulting in drought in 30,583 villages. In 2002, the rainfall amount was just 173 mm during the monsoon period drought in 41,000 villages (Khera 2006). The country receives substantial annual rainfall during the summer monsoon (June to September) (75 to 80%) (Das and Bhattacharya 2018; Roy et al. 2022). The yearly Indian Summer Monsoon (ISM) cycle displays seasonal to annual variations over time (Das et al. 2021a; Das 2012; Yin et al. 2016). Consequently, the spatiotemporal distributions and variations of Indian monsoon rainfall are a governing factor in case of occurrences of drought (due to deficiency of rainfall) or flood (due to excessive rainfall) (Mitra and Das 2022; Yin et al. 2016, Mitra et al. 2022; Poddar et al. 2023). The peninsular and western parts of India are mainly affected by drought. Droughts have been particularly severe in India's western regions (Rajasthan and Gujarat provinces) due to an insufficient and late monsoon, abnormally high temperatures, especially in the summer, and other adverse meteorological conditions. Drought is a recurring natural phenomenon in Rajasthan, including the largest Luni River Basin (LRB) and mild droughts were more likely than moderate and severe droughts to cause severe drought (Mundetia and Sharma 2015). Moreover, Chhajer et al. (2015) investigated the spatiotemporal characteristics of drought in Jaisalmer, Rajasthan, using SPI and other indices.

A number of drought indices have been devised to describe the drought (Citakoglu and Coşkun 2022; Uddin et al. 2020; Demir 2022; Demir et al. 2020; Akturk et al. 2022). An extensively used index, the standardized precipitation index (SPI), measures an area's meteorological drought status which relies on rainfall probability at any

point in time scale (Alsubih et al. 2021). The findings of SPI were evaluated widely for the several climatic zones of the world, with varying results, such as in wet and desert zones (Czerniak et al. 2020). Analysis of trends is necessary to investigate the drought pattern and adapt some measures priorly so we can combat the effects of drought and its complexity. However, it is common practice to investigate the trend pattern using the Mann-Kendall (MK) test (Mann 1945; Kendall 1975), the modified Mann-Kendall (mMK) test (Gupta et al. 2023; Mandal et al. 2021a, b; Yue and Wang 2004), and a recently developed graphical innovative trend analysis (ITA) test (Şen 2012). The popular and most widely used MK test has some flaws, which is why researchers are currently adopting approaches like the mMK-test and the ITA test to address these flaws (Basak et al. 2021; Mandal et al. 2022; Mallick et al. 2021). Şen (2012) suggested the widely utilized ITA in the research field of water resources. A few researchers have used this newly developed technique to investigate rainfall differences in various locations of the world (Caloiero 2020), and very few researchers have used this newly developed technique to investigate the non-monotonic as well as the hidden trend of drought, whereas MK test can detect only monotonic trend.

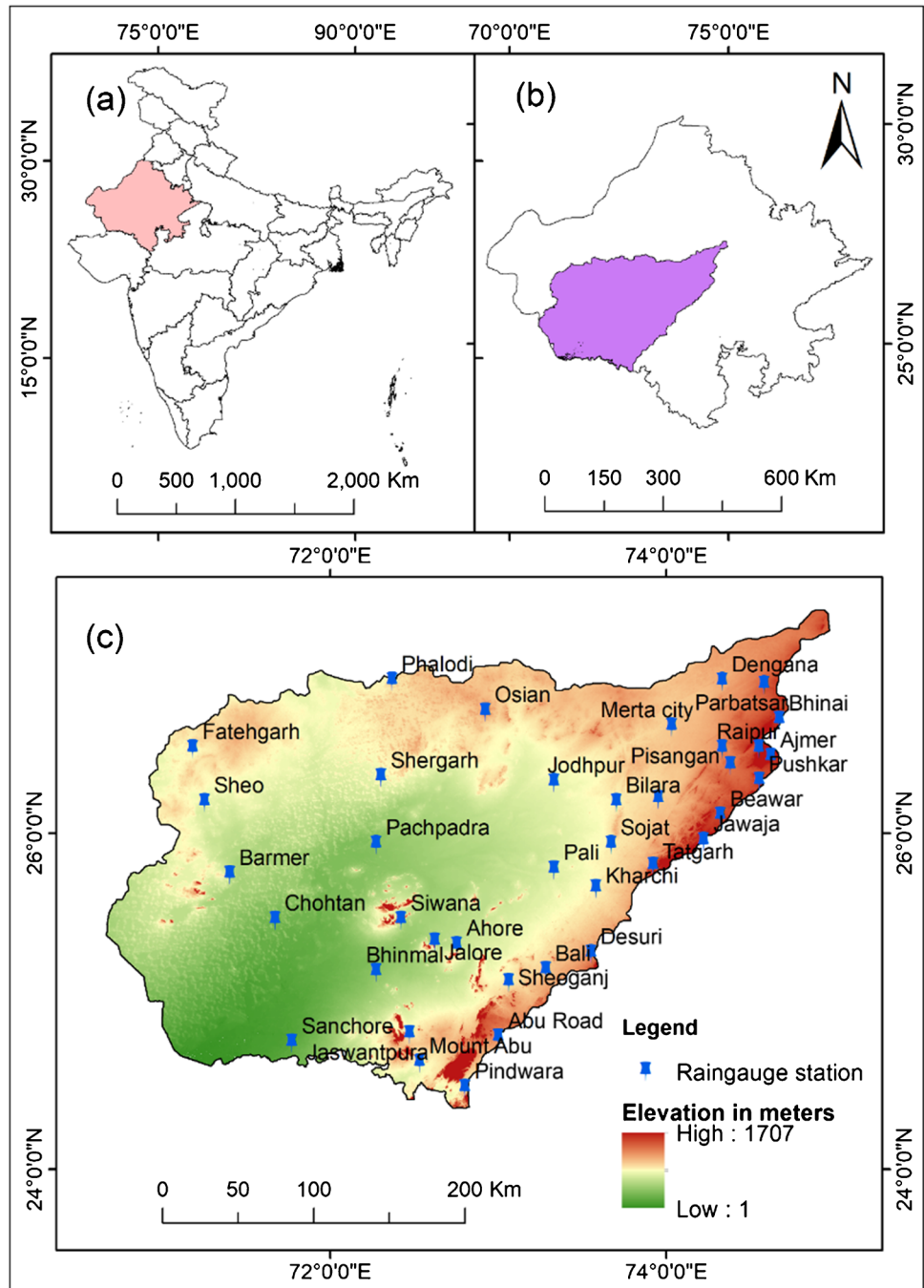
The drought scenario was the main subject of this investigation over the Luni basin using the standardized precipitation indexes (SPI 3, SPI 6, SPI 12, and SPI 24) and focused on occurrences of meteorological-drought episodes using the rainfall data from 1959 to 2019. Among all the standardized drought measures, based on McKee et al. (1993), Dehghani et al. (2014), this study employed the SPI (Caloiero 2020; Zhao et al. 2020; Achour et al. 2020) for analysis purposes. In this kind of study, non-parametric tests are superior to parametric methods for dealing with non-normally distributed hydrometeorology (Golian et al. 2015; Benzater et al. 2021). The frequency and trends (MK, mMK, and ITA) of SPI values were employed as the main drought indicators for this purpose. The spatial behavior of drought frequencies in the river basin is also discussed throughout the research. The application of the ITA approach to investigate the drought trend over the LRB has been first employed by researchers in this case study. It has never been the subject of any previous inquiry in this region; therefore, the study is unique in its nature and dimensions. The inclusion of the ITA graph is reliable to show the present investigation. The comparison of MK, mMK, and ITA outcome for the desertic region of India manifests the interesting part of the research. This study also mentions the impact of the IOD and ENSO with the SPI of LRB and tries to relevant their interconnections. Hydro-climatic understanding and early warning of imminent drought in this region could be improved with the help of this research, and the severity of drought could be controlled by following the analysis.

Description of the study area

Drought has been a regular phenomenon in Rajasthan for decades (Das et al. 2020a, b). Drought is linked to a lack of rainfall along with high temperatures in Rajasthan, India. As a result, Rajasthan experienced a severe drought in 2001 that affected 30,583 villages, and in 2002, 41,000 villages experienced a similar condition (Ganguli and Reddy 2013). The Aravalli range, one of India’s leading mountain

ranges, acts as a deterrent between Thar Desert’s western reaches and the Malwa Plateau’s eastern plains. Moreover, the south-westerly monsoon wind, on the other hand, clashes with the Aravalli range regularly, causing rain showers on the range’s eastern side and transforming the western side into a rain shadow zone. The current research is an identification of drought trend over the Luni basin is located between 24°30’00” N and 27°10’00” N latitudes and 71°15’34” E and 75°48’18”E longitudes and spans a large region of 78,380 km² to the-west of the-Aravalli

Fig. 1 Location map of the study area. **a** The spatial location of Rajasthan in India, **b** location of Luni basin in Rajasthan, **c** position of the 39 rain gauge stations of the Luni basin



in the rain-shadow-zone (Fig. 1). The Aravalli hard-rock hills in the east and a gently sloping little alluvial plain in the west form the boundaries of this basin. However, near Ajmer on the western sides of the the-Aravalli-ranges, the Luni River rises to a height of -772.0 m above the msl and flows for 511 km in a southwesterly in Rajasthan until merging with the Rann of Kachh. In addition, This Luni basin receives an average of 320 mm of yearly rainfall, with 91% of that falling during the monsoon period. However, as the intensity and amount of rainfall distribution fluctuate during the crop-growing season, the region shows great variations in the start of sowing (Kumar and Jain 2011), and it is also noted for its intense heat in the summer. Summer temperatures range from 40 to 35°C when it rains, while winter temperatures are 10°C, according to the Bureau of Meteorology. In the research area, the mean annual rainfall distribution has reduced from-eastern to the western side. The Aravalli Mountain range has a critical influence on the incidence of drought in this river basin. Because of the monsoon breeze, rainfall occurs primarily from June to September in this area, where the non-monsoon rainfall is limited or intermittent.

The main constraining barrier to agricultural productivity in the region is the insufficient moisture content of the soil. The condition of the groundwater is comparatively low across the basin. These limitations result in the basin's agriculture not being of the highest standard or very economical. Nevertheless, double cropping is used in some locations beside river banks wherein generally excellent quality water is accessible at relatively shallow depths. Rainfed agriculture is feasible on the bulk of the ground. The main products

within fine-textured soil include jowar, maize, and gram. Wheat, rayada, rijika, and other grains are produced on land with a marginally fine texture. Bajra, til, mung, and guar are the main commodities cultivated in medium-textured soil, while bajra, guar, moth, and mung grow in coarse-textured soil. The LULC map of the study area demonstrates six categories of land use practices over the study area in Fig. 2. Most of the areas are covered with rangelands and agricultural lands.

Materials and methods

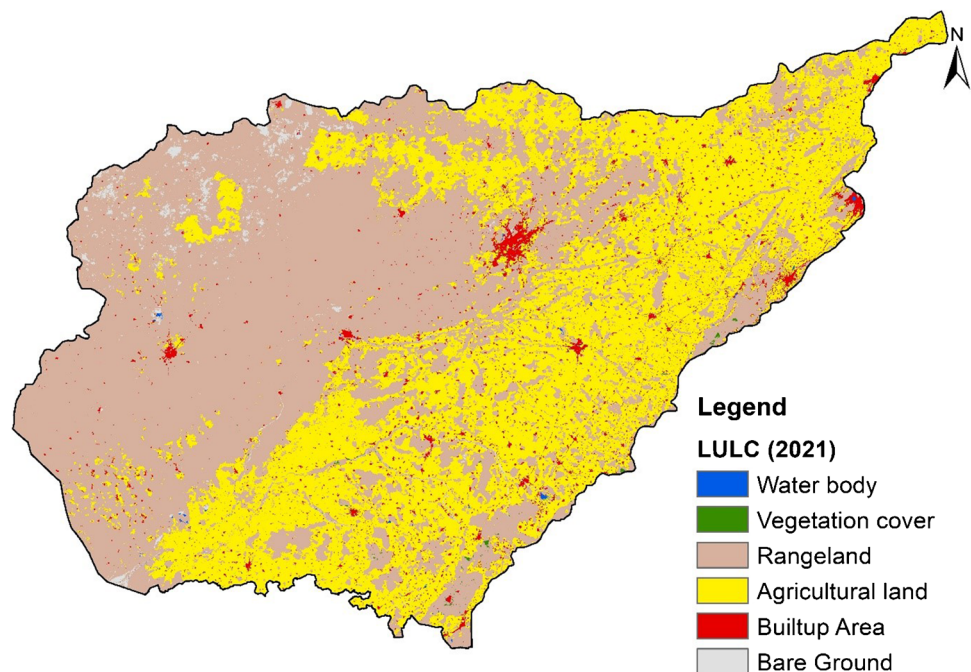
Rainfall data from 39 sites of the Luni River basin during 1959–2019 was used in the proposed study. The observational rainfall records were evaluated using the Water Resources Department's archives of Rajasthan. Some of the stations, however, were deleted because of missing data (about 1%), which was computed using the multiple imputation approach.

Moreover, ClimDex version 1.3 was utilized in the study to ensure data quality. There were two methods used to check for the quality of the data:

- (a) Typographical error (i.e., “0” instead of “O”)
- (b) Values

For LULC map preparation, the research used Sentinel-2 satellite data, and the supervised classification method (maximum likelihood algorithm) was performed based on studies by Mitra and Roy (2022), Saha et al. (2022), and

Fig. 2 Land use and land cover map of Luni basin



Hlanze et al. (2023). The data of SOI (ENSO) and IOD (DMI, dipole mode index) for the period 1901–2015 were collected from <http://www.bom.gov.au/climate/current/soihtm1.shtml> website.

Homogeneity is crucial in climate-based analyses. Inhomogeneity in a dataset causes numerous concerns (biased trends, abrupt discontinuities in the dataset). To solve these difficulties, homogeneity testing is utilized based on Das et al. 2019. ArcMap 10.3 and R 3.6.1 softwares were used for the mapping and data analysis, respectively, and the kriging approach was chosen for interpolation. The following sections provide descriptions of the various methodologies employed in this investigation.

Standardized precipitation index (SPI)

McKee et al. (1993) provide the SPI, which was computed for monitoring meteorological drought in the study area on a 3, 6, 9, 12, and 24-month period. On different time scales, this index can provide a precise summary of the degree of moisture or dryness (Basak et al. 2022). There are two steps in this process:

- (a) Fitting a probability density function (PDF) to observe the relative frequency distribution of rainfall averaged over the desired time scale (PCm)
- (b) Standardizing normal probability distribution functions (PDFs) from each probability distribution function (Dabanli et al. 2017)

The gamma distribution was expressed using the probability function:

$$g(x) = \frac{1}{\beta^\alpha \Gamma(\alpha)} x^{\alpha-1} e^{-x/\beta} \tag{1}$$

Parameter appearance is explained by α . The parameter's range is denoted by β , rainfall is represented by x , and the gamma function is represented by $\Gamma(\alpha)$. The values of α and β parameters are >0 . Here, the gamma-function $\Gamma(\alpha)$ can be written as follows:

$$\Gamma(\alpha) = \lim_{n \rightarrow \infty} \prod_{v=0}^{n-1} \frac{n! n^{y-1}}{y+v} \equiv \int_0^\infty y^{\alpha-1} e^{-y} dy \tag{2}$$

The parameters $\hat{\alpha}$ and $\hat{\beta}$ must be computed to adjust the gamma distribution. To accurately obtain $\hat{\alpha}$ and $\hat{\beta}$, maximum probability solutions are employed as follows (Thom 1958):

$$\hat{\alpha} = \frac{1}{4A} \left(1 + \sqrt{1 + \frac{4A}{3}} \right) \tag{3}$$

$$\hat{\beta} = \frac{x}{\hat{\alpha}} \tag{4}$$

where

$$A = \ln(\bar{x}) - \frac{\sum \ln(x)}{n} \tag{5}$$

Then, to find out the growing probability-distribution-function $G(x)$ of a certain time scale, the $\hat{\alpha}$ and $\hat{\beta}$ parameters are used as follows:

$$G(x) = \int_0^x g(x) dx = \frac{1}{\hat{\beta}^{\hat{\alpha}} \Gamma(\hat{\alpha})} \int_0^x x^{\hat{\alpha}} e^{-x/\hat{\beta}} dx \tag{6}$$

The preceding equation can be simplified by replacing $x/\hat{\beta}$ with t .

$$G(x) = \frac{1}{r(\hat{\alpha})} \int_0^x t^{\hat{\alpha}-1} e^{-t} dt \tag{7}$$

The rain does not fall in a steady stream. When there is no rain, the execution of zero-value must be explained. According to Edwards (1997), real non-exceedance $H(x)$ feasibility can be reckoned as follows:

$$H(x) = q + (1 - q)G(x) \tag{8}$$

where q represents the probability of a zero-event and the recurrence of zeros in a rainfall time series dataset. Thom (1958) proposes a mathematical formula for calculating q :

$$q = \frac{m}{n} \tag{9}$$

The latest SPI program, produced by Nebraska University's National Drought Mitigation Center, has been used to investigate this present study. The SPI severity of the drought classes is presented in Table 1.

Table 1 Classification of climate according to the standardized precipitation index (SPI) values (McKee et al. 1993; Buttafuoco et al. 2015; Das et al. 2020a, b; de Brito et al. 2021)

SPI value	Class	Probability (%)
$SPI \geq -2.00$	Extremely-wet	2.30
$1.5 \leq SPI < 2.00$	Severely-wet	4.40
$1.0 \leq SPI < 1.50$	Moderately-wet	9.20
$SPI < -1.00$	Mildly-wet	34.10
$-1.00 \leq SPI < 0.00$	Mild-drought	34.10
$-1.50 \leq SPI < -1.00$	Moderate-drought	9.20
$-2.00 \leq SPI < -1.50$	Severe-drought	4.40
$SPI < -2.00$	Extreme-drought	2.30

Autocorrelation function

Autocorrelation is generally of the main obstacles to trend detection in time series. The dispersion of the MK test statistic increases the level of sequential reliance. Additionally, positive serial interdependence in a time series dataset enhances the type I error (false positive) and identifies a trend that is substantial even while it is not a true trend. This study utilized the autocorrelation function based on Das et al. (2021b).

Mann-Kendall (MK) test

There are several different methods for assessing trends In the literature. However, in hydroclimatic investigations, the MK test is extensively employed for evaluating trends (Piniewski et al. 2018). The MK test was conferred by The WMO (World Meteorological Organization), which has a number of benefits (Şen 2012; Kuriqi et al. 2020). The following equations can be used to construct the MK test. In Eq. (10), n denotes the size of the sample, whereas x_p and x_q denote consecutive data within a series.

$$S = \sum_{i=1}^{n-1} \cdot \sum_{j=i+1}^n \text{sign}(x_p - x_q) \tag{10}$$

where x_k and x_i are sequential data in the series.

$$\text{sign}(x_p - x_q) = \begin{cases} +1 & \text{when } (x_p - x_q) > 0 \\ 0 & \text{when } (x_p - x_q) = 0 \\ -1 & \text{when } (x_p - x_q) < 0 \end{cases} \tag{11}$$

The variance of S is estimated as

$$\text{Var}(S) = \frac{s(n - 1)(2n + 5) - \sum_{p=1}^q tp(t_p - 1)(2t_p + 5)}{18} \tag{12}$$

whereas tp and q denotes the number of ties for the p value. Equation (13) shows how to calculate the Z statistic, the standardized test for the MK test (Z):

$$Z = \begin{cases} \frac{s-1}{\sqrt{\text{Var}(S)}} & \text{when } S > 0 \\ 0 & \text{when } S = 0 \\ \frac{s+1}{\sqrt{\text{Var}(S)}} & \text{when } S < 0 \end{cases} \tag{13}$$

The trend’s direction is indicated by the letter Z . A negative Z value indicates a diminishing trend and vice versa. Trends were examined in this study using a significance threshold of $\alpha = 0.05$. When the absolute value of Z exceeds 1.96, the critical Z value at 95% two-tailed confidence interval, the null hypothesis of no trend is rejected. The Mann-Kendall (MK) test has been applied to identify the importance of the variation in monthly rainfall.

Modified Mann-Kendall test

The modified Mann-Kendall (mMMK) test has been conducted in this research based on Das et al. (2021b). The following equation is the expression of mMMK:

$$\text{VAR}(S) = \frac{n(n - 1)(2n + 1)}{18} \cdot \frac{n}{n_e^*} \tag{14}$$

Innovative trend analysis

Şen (2012) has proposed the use of ITA for the first time to identify trends in the time series data. However, in this condition, firstly, the data is evenly partitioned into two pieces from the start to the latest date in this method (Kuriqi et al. 2020). To get the scatter template, secondly, plot the sub-series against each other, then place the first half along the horizontal axis and the second half along the vertical axis. To portray trendless in a time series dataset, draw the 1:1 (45°) straight line in the third sta

ge. If the scatter points aggregate above or below the 1:1 (45°) straight line, the hydro-meteorological time series shows a rising or declining trend (Şen 2012). At a 90% confidence level, the exponent is multiplied by ten to attain a similar scale as MK (Mann-Kendall) test analysis and Sen’s slope estimator, allowing direct comparison (Ahmad et al. 2018). Consequently, the ITA (Şen 2012) indicative is constructed as below:

$$B = \frac{1}{n} \sum_{i=1}^{i=n} \frac{10(x_j - x_k)}{\bar{x}} \tag{15}$$

where x_j and x_k are the first- and second-half values of the subseries, respectively. Moreover, the mean of the first half is x , and B is a trend indicator. A positive value of B implies a rising time series, whereas a negative B value suggests that it is falling. Suppose the recorded original time series has an unusual. In that case, the very first observation is omitted before it is separated into two halves, allowing the more recent period data to be completely utilized.

Mapping of the drought trends using GIS

Spatial patterns of drought trends have been manifested using the ArcGis software. For this, we first computed the SPI in the excel sheet, and then Z statistic and ITA type have been assigned. After that, using the base map of the study area, we added the XY data in ArcGIS. Using the “IDW” technique, the mapping has been completed. Thus, this research integrates GIS to show the spatial pattern of drought trends in the LRB.

Graphical representation of the data

The long-term annual rainfall data of the LRB has been shown with Box and whisker plots diagram by employing GraphPad Prism software. In this study, the graphical representation of the SPI data has been prepared using GraphPad Prism and MS Excel softwares. The GraphPad Prism was used to plot the variations of monthly rainfalls at different SPI time scales for 39 stations. For this, at first, the data were opened in GraphPad Prism and then selected the “Grouped: Heat map” option of graphs. After finalizing the “Color mapping,” “graph setting,” “Titles,” “Labels,” “Gaps,” and “Legend” in the Format Graph dialog box, the heat map of monthly rainfall has been obtained. The MS Excel software was utilized to demonstrate the different types of drought frequency in the LRB based on selected SPI time scales. In MS Excel, first, insert the data, and then open the “3D Map” option of the Insert function. In the “3D Map” section, first, select the “Heat map” option and finalize all the needed layers for the current study. After the calculation of the ITA graphs in R software, the data were represented using MS Excel software.

Results

The main objective of this study was to find a probable drought trend in the LRB for the period of 1959 to 2019. The data were analyzed applying some non-parametric statistical tests, for example, Mann-Kendall (MK) and modified Mann-Kendall (mMK), standardized precipitation index (SPI) was analyzed to monitor the drought events in various time scales (SPI 3, 6, 12, and 24 time scales). Moreover, one of the newly developed Sen’s Innovative trends has been adopted to investigate non-monotonic drought trends where MK and mMK can only detect monotonic trends.

Rainfall pattern in LRB

One of India’s most water-scarce river basins is the Luni River Basin, which is distinguished by exceptionally high aridity and very little rain in most areas. Before assessing the drought trend in terms of space and time, it is required to conduct an initial review of rainfall data (Haktanir and Citakoglu 2015; Yagbasan, et al. 2017). The ability to check the trend and skewness of the rainfall trend over the Luni basin in Rajasthan is the goal for adopting this method. The descriptive statistics of the annual rainfall of 39 selected stations of the LRB are analyzed and presented in Table 2. Based on Table 2, the highest mean (1588.96) and SD (744.46) of annual rainfall have been observed in Mount Abu, where the lowest mean (177.44) in Fatehgarh and SD (107.18) in Phalodi station. The maximum CV (105.16),

skewness (5.24), and kurtosis (34.20) were found in Shergarh, and minimum CV (35.47), skewness (0.00), and kurtosis (−0.72) were found in Ajmer, Tatgarh, and Beawar, respectively. The box-plot method can compare numerous datasets side by side, as shown in Fig. 3. This graph shows a significant variation in annual rainfall over 39 locations for the whole study period. Mount Abu station has the greatest temporal fluctuation, with an inter-quartile range (IQR) of roughly 900 mm/year. Phalodi had the smallest variations in time, followed by Fategarh, Barmer, and Sheo. These stations’ interquartile range is roughly 200 mm/year on average. The remaining sites had IQR values of 400–800 mm/year, which were remarkably similar in annual rainfall temporal changes. A comparable comparison of annual rainfall intensity has also been noticed by this box-plot technique. The maximum rainfall intensity was noticeable at Mount Abu, Aburoad, Desuri, Pindwara, and Sirohi stations, where the long-term average value for Mount Abu is 1200 mm/year, and the remainder of the three stations is 600 mm/year. Barmer, Fategarh, Phalodi, and Sheo stations experienced the least amount of annual rainfall. These stations’ average annual rainfall was roughly 200 mm. A few median lines in the boxes are also next to either the top or bottom horizontal lines. The length of the upper fences is unequal to the length of the lower fences, indicating that rainfall data series at a number of locations fail to meet the basic premise of normal distribution. As a result, a non-parametric approach is required to analyze rainfall trends.

Drought characteristics in LRB

The spatio-temporal analysis of the meteorological drought in the LRB has been conducted for 39 places. Based on different SPI time scales (3, 6, 12, and 24), the monthly rainfall has been depicted through a heat map in Fig. 4. The map was prepared to compare the short-term SPI (SPI 3 and SPI 6) and long-term SPI (SPI 12 and SPI 24) in the LRB. The temporal pattern of monthly rainfall in the SPI 3 scale manifests that except for the stations Pachpadra, Jaitaran, Fatehgarh, Bhinai, and Barmer, most of the station experienced dryness. On the basis of the SPI 6 and 12 scale, Sheoganj is the driest station, and Pachpadra, Jaitaran, and Bhinai are the wettest stations. The long-term SPI scale (SPI 24) represents only Pachpadra is the wettest station among the 39 stations. In this study, the heat map technique is again utilized to show the different types of droughts frequencies in the LRB based on SPI 3, 6, and 24 time scales. The types of droughts have been classified into four categories, i.e., extreme, severe, moderate, and mild. In Supplementary Material (SM) 1, different types of drought frequencies were tabulated. The highest frequency (761) of extreme drought events has been found in SPI 24, and the lowest frequency of

Table 2 Descriptive statistics of annual rainfall

Station	Lat.	Long.	Mean	Standard deviation (SD)	Coefficient of variation (CV)	Skewness	Kurtosis
Abu Road	24.78	72.998	686.62	349.70	50.93	0.73	0.12
Ahore	25.33	72.75	398.82	179.56	45.02	0.43	-0.11
Ajmer	26.45	74.62	545.67	193.56	35.47	0.77	0.66
Bali	25.18	73.28	587.93	282.20	48.00	1.34	3.01
Barmer	25.75	71.4	277.84	167.51	60.29	0.88	0.74
Beawar	26.1	74.32	560.48	212.01	37.83	0.34	-0.72
Bhinai	26.67	74.67	464.44	236.54	50.93	0.08	-0.30
Bhinmal	25.17	72.27	431.32	242.61	56.25	0.65	-0.13
Bilara	26.18	73.7	436.55	196.06	44.91	1.24	2.67
Chohtan	25.48	71.67	295.36	184.21	62.37	1.01	0.76
Dengana	26.9	74.33	427.18	232.03	54.32	2.64	11.93
Desuri	25.28	73.55	650.83	291.81	44.84	1.04	1.62
Fatehgarh	26.5	71.18	177.44	128.47	72.40	0.72	-0.14
Jaitaran	26.2	73.95	425.38	187.74	44.13	0.55	-0.29
Jalore	25.35	72.62	434.12	234.65	54.05	0.90	0.01
Jaswantpura	24.8	72.47	484.22	292.31	60.37	0.67	-0.40
Jawaja	25.95	74.22	416.03	226.89	54.54	0.32	-0.29
Jodhpur	26.3	73.33	373.82	164.41	43.98	0.48	-0.47
Kharchi	25.67	73.58	482.87	251.22	52.03	0.16	-0.66
Mangaliawas	26.308	74.551	345.28	209.57	60.70	0.70	0.30
Merta city	26.63	74.03	398.09	180.18	45.26	0.88	0.60
Mount Abu	24.63	72.53	1588.96	744.46	46.85	0.77	0.23
Osian	26.72	72.92	305.58	118.65	38.83	0.38	-0.40
Pachpadra	25.93	72.27	261.84	138.50	52.90	0.51	-0.59
Pali	25.78	73.33	433.36	221.31	51.07	0.75	-0.12
Parbatsar	26.88	74.58	439.43	223.96	50.96	0.93	0.55
Phalodi	26.902	72.366	233.53	107.18	45.89	0.82	0.67
Pindwara	24.48	72.8	716.94	368.25	51.36	1.56	3.35
Pisangan	26.4	74.38	426.67	203.48	47.69	0.38	-0.22
Pushkar	26.5	74.55	459.26	253.33	55.16	0.57	0.33
Raipur	26.5	74.33	502.98	210.59	41.87	0.32	-0.45
Sanchore	24.75	71.77	409.75	261.94	63.93	0.74	-0.34
Sheo	26.18	71.25	232.16	112.52	48.46	0.48	-0.25
Sheoganj	25.11	73.06	520.23	267.34	51.39	1.44	4.86
Shergarh	26.33	72.3	369.06	388.10	105.16	5.24	34.20
Sirohi	24.88	72.86	621.17	313.82	50.52	1.01	0.82
Siwana	25.48	72.42	369.46	210.42	56.95	1.11	1.12
Sojat	25.93	73.67	425.88	200.54	47.09	0.71	0.30
Tatgarh	25.801	73.92	501.74	231.66	46.17	0.00	-0.28

extreme drought events (203) has been confined in SPI 3. For SPI 6 and SPI 12, the frequencies of extreme drought events are 369 and 686, respectively. The spatial pattern of distribution in this river basin has been illustrated on the basis of short-term SPI (SPI 3 and SPI 6) and long-term SPI (SPI 24) in Figs. 5, 6, and 7. The heat map technique is utilized to present the data. Table 3 gives a clear picture of

the station-wise duration of meteorological drought years from 1959 to 2019. Fatehgarh has the maximum experience of drought as it occurred in 31 years between 1959 and 2019, followed by Aburoad (29 years), Beawar (27 years), and Pindwara (25 years). Phalodi has minimum experience (11 years) of drought phenomena.

Fig. 3 Box and whisker plots of annual rainfall for the Luni River basin (1959–2019)

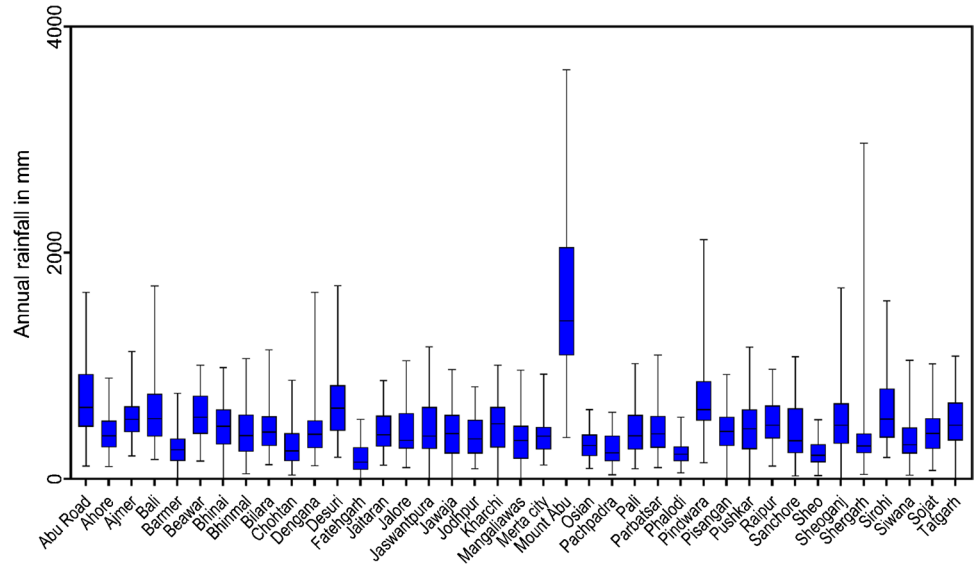
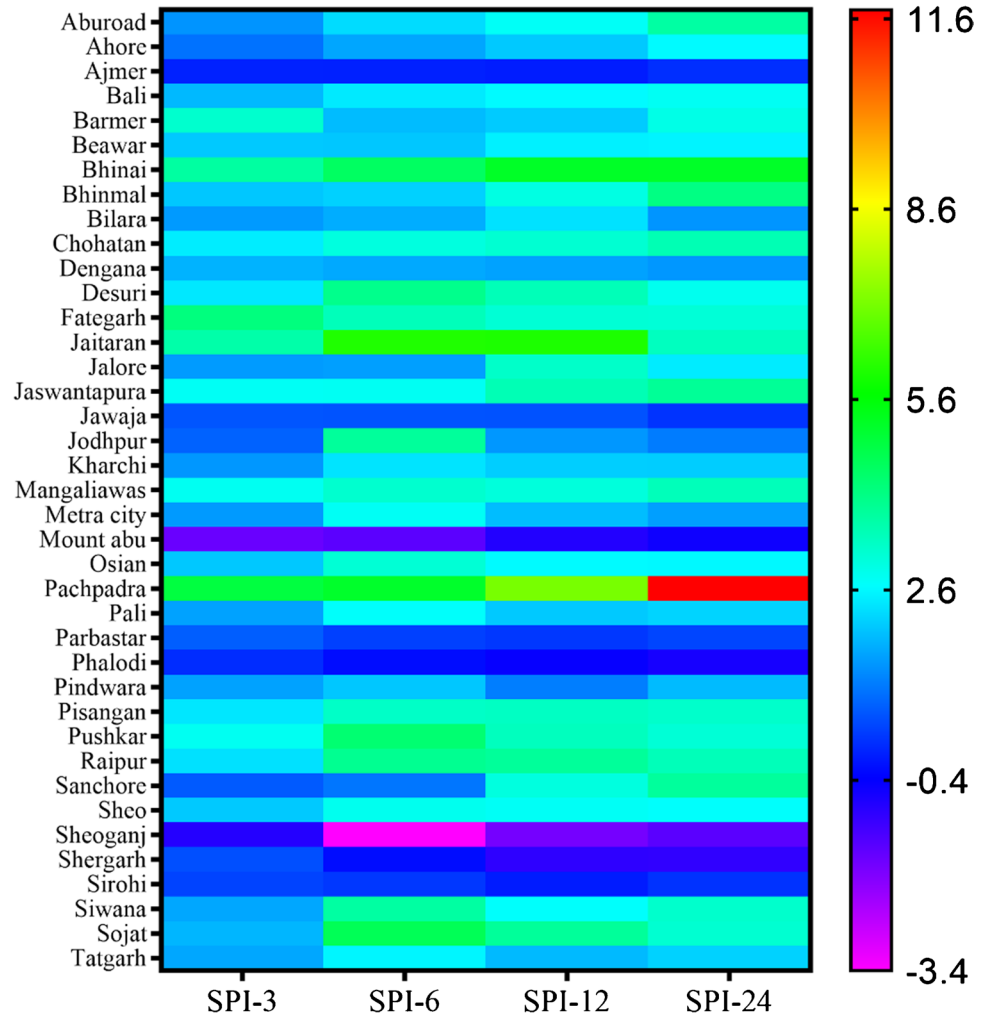


Fig. 4 Plotting of monthly rainfalls at different SPI time scales for 39 stations



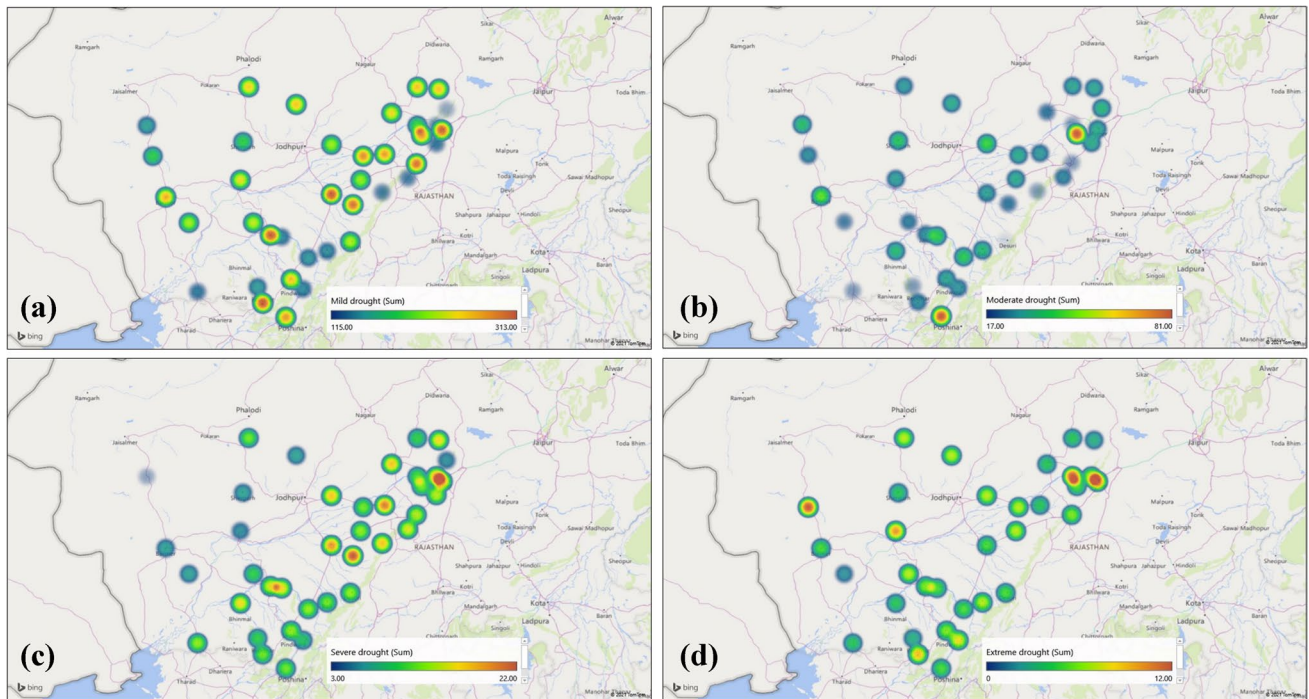


Fig. 5 Different types of drought frequency in the Luni River basin based on SPI 3: **a** mild drought, **b** moderate drought, **c** severe drought, and **d** extreme drought

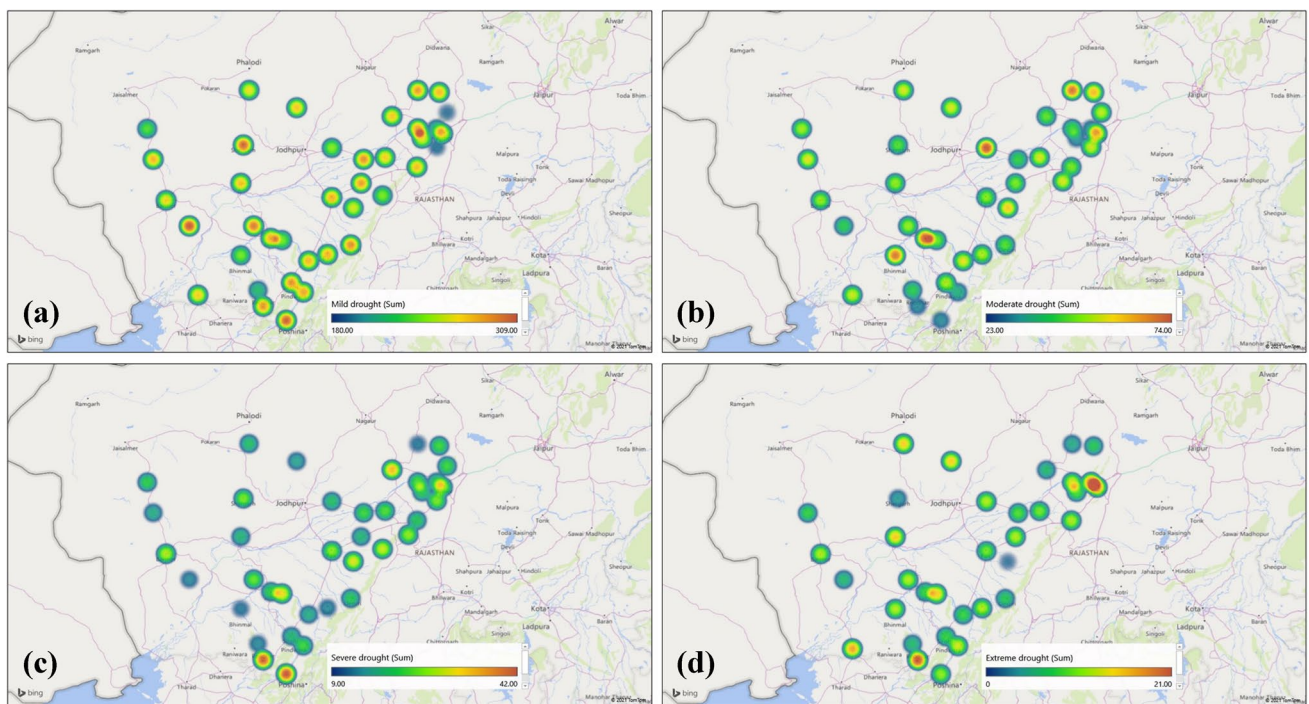


Fig. 6 Different types of drought frequency in the Luni River basin based on SPI 6: **a** mild drought, **b** moderate drought, **c** severe drought, and **d** extreme drought

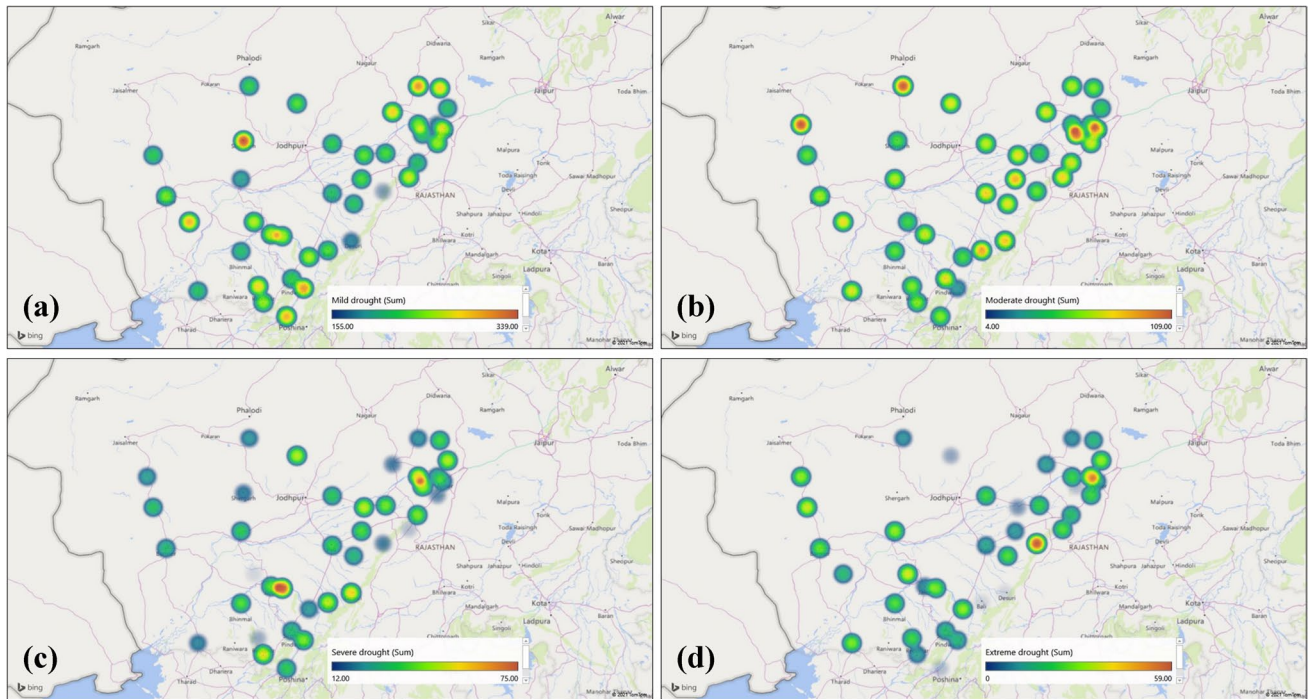


Fig. 7 Different types of drought frequency in the Luni River basin based on SPI 24: **a** mild drought, **b** moderate drought, **c** severe drought, and **d** extreme drought

Relation between SPI, ENSO, and IOD in LRB

The relationship between SPI, El Nino-Southern Oscillation (ENSO), and Indian Ocean Dipole (IOD) has been conducted for this study area to assess their effects on meteorological drought events. Owing to its capacity to alter the worldwide air circulation, which in turn affects worldwide temperatures and precipitation, ENSO is considered one of the foremost significant climate occurrences. Both the ENSO and IOD have an effect on drought and floods in the Indian subcontinent. Their relation in the case of the most significant drought-prone region of the country was here analyzed during the time frame of 1901 to 2015. The SOI may be expressed as a whole number and has a variation of roughly -35 to around $+35$. The SOI is most often generated on a monthly basis, while figures over extended time spans, like an entire year, are occasionally applied. In the ENSO data, El Nino events are frequently indicated by negative SOI values less than -7 , while a La Nia incident typically has SOI values that are more than $+7$.

By adopting the partial correlation statistical technique, the relationships have been judged at 95% and 99% confidence levels. In SM 2 and SM 3, the excel tabulation sheets of partial correlation between SPI, IOD, and ENSO have been illustrated. In Table 4, C_ENSO+IOD indicates that the IOD is the main variable and ENSO is the control variable, while C_IOD+ENSO represents that the ENSO

is the main variable and IOD is the control variable. In the C_ENSO+IOD column, there are observed positive correlations in 14 stations between the observed SPI and IOD in the LRB, and a negative correlation in the rest of all stations. The ENSO acts as the catalyst and affects the entire region. The spatial pattern of the effects of IOD in the SPI over this basin manifests some areas are substantially impacted by it. The impacted stations are as follows: Bali, Barmer, Bhinai, Fatehgarh, Jaswantapura, Mangaliawas, Metra city, Pali, Parbastar, Phalodi, Pindwara, Pisangan, Pushkar, and Shergarh. Mainly, the north-eastern, eastern, south-eastern, and northern parts of the basin are impacted by the IOD. The Mangaliawas station has a significant positive correlation (0.037) among the variables SPI and IOD at a 95% confidence level (2-tailed) in 705 degrees of freedom. The station Osian and Tatgarh show a significant negative correlation at a 95% confidence level (2-tailed) between SPI and IOD. In the C_IOD+ENSO column, there are found a positive correlation only in two stations between SPI and ENSO, and all other stations show a negative correlation. The two stations, which are impacted by ENSO are as follows: Ahore and Fatehgarh. The Ahore and Fatehgarh are located in the eastern and north-eastern parts of the LRB; therefore, ENSO has an impact on some small patches of the basin. The stations Pisangan, Osian, Mount Abu, Kharchi, Dengana, Barmer, Ajmer and Parbastar, Phalodi, Pushkar, and Metra city

Table 3 Identifying the drought years and frequencies of the Luni basin for the period of 1959–2019

Station	Drought years	Duration (years)
Abu road	1959, 1964–1968, 1969–1973, 1975, 1982–1984, 1986–1988, 1990, 1992, 1994, 2003, 2005–2006, 2010, 2013, 2019	29
Ahore	1959, 1962–1964, 1966, 1968–1971, 1981–1982, 1986–1991, 2000–2006	24
Ajmer	1960–1961, 1964, 1966–1967, 1969–1970, 1973, 1981–1982, 1986–1991, 2000–2006	21
Bali	1959–1961, 1963–1964, 1969–1971, 1979, 1993, 2007, 2011–2013	14
Barmer	1964, 1966, 1968–1973, 1980–1981, 1986–1988, 2000, 2009	15
Beawar	1959–1964, 1970, 1973–1974, 1978, 1982, 1985–1990, 1992–1994, 2000–2001, 2003, 2005, 2007, 2010, 2014–2015	27
Bhinai	1959–1961, 1964–1966, 1968, 1972–1974, 1980–1989, 2009	21
Bhinmal	1962–1963, 1967, 1969–1970, 1981, 1985–1989, 1999, 2001–2002	14
Bilara	1959–1962, 1964, 1966, 1968–1970, 1973, 1981, 1986–1987, 2001–2003, 2009–2010	17
Chohtan	1960–1961, 1963–1964, 1967–1968, 1969–1970, 1979, 1981, 1984–1987, 2000, 2005	16
Dengana	1960–1962, 1964, 1966–1968, 1970, 1985–1991, 2002, 2012	16
Desuri	1959–1961, 1963–1964, 1966, 1969–1970, 1973–1974, 1975, 1981–1982, 1985–1987, 1999–2000, 2005, 2009	20
Fatehgarh	1963–1972, 1975, 1978–1979, 1982–1989, 1992	31
Jaitaran	1960–1964, 1967, 1969–1970, 1972–1974, 1981–1982, 1985–1989, 2000, 2003	20
Jalore	1959–1960, 1962–1966, 1968–1970, 1976, 1981–1982, 1986–1989, 2001–2005, 2009	23
Jaswantpura	1962–1965, 1967, 1969–1970, 1972–1974, 1976, 1981–1982, 1985–1989, 1996, 1999–2000	19
Jawaja	1960–1961, 1963–1964, 1966–1969, 1972, 1986–1988, 2008–2011, 2016	17
Jodhpur	1960–1961, 1963–1965, 1969–1970, 1972, 1974, 1981, 1985–1989, 2005–2007	18
Kharchi	1960–1961, 1963–1966, 1969–1970, 1972, 1975, 1985, 1988, 1998, 2006	14
Mangaliawas	1962–1965, 1967–1970, 1973, 1975, 1978–1980, 1982, 1986–1993	22
Merta City	1961, 1964, 1966–1971, 1974, 1981–1982, 1986–1989, 2001–2003	17
Mount Abu	1963–1964, 1966–1967, 1969–1970, 1975, 1981–1984, 1985–1987, 1990, 1996, 1999–2004, 2009–2010, 2015, 2016, 2019	26
Osian	1960–1961, 1963–1965, 1969–1970, 1986–1989, 2000, 2006–2009	16
Pachpadra	1959–1961, 1963–1966, 1969–1970, 1973–1974, 1978, 1981, 1985–1989	18
Pali	1959–1961, 1963–1964, 1969–1970, 1973, 1981–1982, 1984–1987, 1999–2000, 2003–2005, 2009	20
Parbatsar	1960–1962, 1964–1966, 1969, 1985–1991, 1994, 1999–2000, 2005–2007	19
Phalodi	1960–1961, 1964, 1969–1973, 1988–1989, 2000, 2005	11
Pindwara	1963–1964, 1966–1970, 1973–1975, 1981–1983, 1985–1989, 1999, 2000–2003, 2009–2010, 2015, 2019	25
Pisangan	1959–1961, 1963, 1966–1970, 1974–1975, 1986–1988, 1992, 2009	16
Pushkar	1963–1964, 1966–1970, 1974–1975, 1986–1988, 1992, 2009	15
Raipur	1961, 1963, 1965, 1968–1970, 1972–1973, 1981–1984, 1986–1988, 2000, 2003–2004	21
Sanchore	1961, 1963–1964, 1966–1970, 1972–1973, 1975, 1980, 1986–1987, 1999, 2001–2002, 2008–2009	18
Sheo	1961, 1965–1966, 1969–1970, 1975, 1978, 1981–1991	18
Sheoganj	1963, 1969–1970, 1973, 1975, 1981–1982, 1985, 1989–1991, 2005, 2009, 2014	14
Shergarh	1959–1962, 1970, 1975–1976, 1981, 1985–1987, 2005–2006	13
Sirohi	1960–1961, 1964–1965, 1969–1970, 1973, 1975, 1981–1982, 1985–1989, 2000, 2009, 2014	18
Siwana	1960–1961, 1963, 1966–1967, 1969–1970, 1973–1974, 1981, 1986–1989, 2000–2002, 2005, 2012	19
Sojat	1960–1961, 1963–1964, 1969–1970, 1973, 1975, 1981–1982, 1985–1988, 2003–2004	15
Tatgarh	1959–1961, 1963, 1969, 1973, 1978, 1986–1987, 1999–2000, 2004, 2008–2009	14

indicate significant negative correlation at 99% and 95% confidence levels (2-tailed), respectively. Therefore, both variables, IOD and ENSO, have an impact on the uncertainty of rainfall in the LRB.

Drought trends in LRB

To study the type of drought trends in the total 39 stations of the LRB of Rajasthan, different SPI time scales

Table 4 Partial correlations between SPI, IOD, and ENSO

Station	C_ENSO+IOD	C_IOD+ENSO
Aburoad	-0.051	-0.041
Ahore	-0.05	0.004
Ajmer	-0.047	-0.109
Bali	0.002	-0.039
Barmer	0.005	-0.11
Beawar	-0.032	-0.065
Bhinai	0.003	-0.026
Bhinmal	-0.033	-0.016
Bilara	-0.044	-0.066
Chohatan	-0.034	-0.05
Dengana	-0.05	-0.136
Desuri	-0.036	-0.034
Fatehgarh	0.022	0.019
Jaitaran	-0.031	-0.061
Jalore	-0.022	-0.009
Jaswantapura	0.02	-0.036
Jawaja	-0.037	-0.046
Jodhpur	-0.051	-0.052
Kharchi	-0.026	-0.111
Mangaliawas	0.079	-0.039
Metra city	0.029	-0.092
Mount Abu	-0.003	-0.102
Osian	-0.086	-0.101
Pachpadra	-0.055	-0.062
Pali	0.023	-0.061
Parbatar	0.004	-0.08
Phalodi	0.005	-0.078
Pindwara	0.04	-0.013
Pisangan	0.016	-0.099
Pushkar	0.032	-0.078
Raipur	-0.017	-0.017
Sanchoe	-0.044	-0.055
Sheo	-0.003	-0.029
Sheoganj	-0.039	-0.035
Shergarh	0.018	-0.033
Sirohi	-0.001	-0.043
Siwana	-0.016	-0.049
Tatgarh	-0.09	-0.068

C_ENSO, control variable ENSO; *C_IOD*, control variable IOD

(SPI 3, 6, 12, and SPI 24) were calculated for the period of 1959 to 2019. The drought trends, viz., monotonic and non-monotonic types, were analyzed based on MK, mMK, and ITA studies on the LRB. Table 5 and Fig. 8 depict the results of trend analysis at several time scales and spatial variations of increasing (positive) and decreasing (negative) trends (including monotonic and non-monotonic types). Sen's ITA graph shows the increasing and decreasing trends in Figs. 9, 10, 11, and 12. The analyses were

judged in 99% and 95% confidence levels and which is also mentioned in Table 5.

Out of the total of 39 rain gauge stations in the SPI 3 time scale, the ITA detected increasing and decreasing trends for the study area. The decreasing trend of the stations Beawar, Sheo, Pach Padra, and Bali. At the same time, Aburoad and Fategarh showed slightly increasing trends, and the rest of the stations did not detect any trend for the 95% confidence level (Fig. 9). In Fig. 8 and Table 5, Z statistics results revealed that excluding the western part and some small patches of the eastern part of the entire study area does not show any significant trend. In comparison, the ITA trend detected 43% of the recorded rain gauge stations observed a non-monotonic negative trend, and more than 23% of the recorded rainfall gauge stations observed a monotonic positive trend. Whereas only 10% showed a non-monotonic positive trend at SPI 3-time scale (Fig. 8). It is clear from Fig. 10 that the stations Pachpadra, Jaitaran, Parbatar, Ajmer, and Jodhpur faced a decreasing trend while Aburoad, Puskar, Jalore, and Sojat have shown an increasing trend. Figure 8b shows the entire study area at SPI 6-time scales monotonic positive trend excluding some parts of the north and south of the study area. Out of 39 recorded rain gauge stations, 16 stations (41%) experienced a non-monotonic negative trend, and 13 stations (33%) experienced a monotonic positive trend (Fig. 8).

The Z statistics of MK and mMK results have shown at SPI 3, SPI 6, SPI 12, and SPI 24 time scales. In SPI 3 time scale, Bewar, Chohtan Jaswantapura, Raipur, and Sojat these five stations have shown significant monotonic positive trends, and the stations Sheo and Osian have shown significant non-monotonic negative trends. At SPI 6 time scale, there were only 3 stations (Sojat, Puskar, and Osian) that displayed a significant non-monotonic positive trend, and the stations Metracity, Pachpadra, Jaitaran, Fategarh, and Desuri revealed significant non-monotonic negative trends at the same time scale at 99% confidence interval. Whereas, at the 12-time scale, the stations, Pachpadra, Raipur, and Sojat experienced a significant non-monotonic positive trend at the 99% confidence interval. At the SPI 24 time scale, Pali, Jalore, and Bewar stations depicted a significant monotonic positive trend at 95% significant intervals. Only stations in Aburoad exposed a significant monotonic negative trend at a 99% confidence interval. Excluding some small patches of the study area, the entire area experienced a monotonic positive trend at the SPI 12 time scale (Fig. 8). In addition, according to the Z statistics results at the same time scale, the Sen's Innovative trends detected not only the monotonic trends, but also the non-monotonic trend as well. More than 70% of the recorded rain gauge stations experienced two types of drought trends: monotonic positive and non-monotonic negative trends, while 13% of the stations recorded non-monotonic negative trends. The stations

Table 5 Trend of SPI values using MK/mMK and ITA methods during 1959 to 2019

Sl	Station	SPI 3		SPI 6		SPI 12		SPI 24	
		Z statistic	ITA type	Z statistic	ITA type	Z statistic	ITA type	Z statistic	ITA type
1	Aburoad	1.38	MPT	2.24*	MPT	2.75**	MPT	3.74**	MNT
2	Ahore	0.98	NMNT	1.59	MPT	2.01*	TTS	2.60**	TTS
3	Ajmer	0.01	TTS	0.00	MPT	-0.04	MPT	0.17	MPT
4	Bali	1.82	NMNT	2.40*	NMNT	2.60**	NMNT	2.78**	NMNT
5	Barmer	3.23**	MPT	1.85	MPT	2.03*	MPT	2.93**	MPT
6	Beawar	2.01*	NMNT	1.99*	NMNT	2.48*	NMNT	2.52*	MPT
7	Bhinai	3.77**	MPT	4.53**	MPT	5.21**	MPT	5.20**	MPT
8	Bhinmal	1.98*	TTS	2.10*	MNT	2.98**	MPT	4.12**	TTS
9	Bilara	1.45	NMNT	1.68	NMNT	2.31*	NMNT	1.39	NMNT
10	Chohatan	2.44*	MPT	3.03**	MPT	3.18**	MPT	3.54**	MPT
11	Dengana	1.75	NMNT	1.63	NMNT	1.54	NMNT	1.42	NMNT
12	Desuri	2.38*	TTS	12.60**	NMNT	3.49**	NMNT	2.84**	MPT
13	Fategarh	4.18**	MPT	3.47**	NMNT	3.15**	MPT	3.13**	MPT
14	Jaitaran	3.67**	NMNT	23.44**	NMNT	6.01**	NMNT	3.41**	NMNT
15	Jalore	1.46	TTS	1.51	MPT	3.29**	MPT	2.43*	MPT
16	Jaswantapura	2.77**	MPT	2.79**	TTS	3.53**	NMNT	3.88**	NMNT
17	Jawaja	0.63	NMNT	0.61	NMNT	0.59	TTS	0.23	NMNT
18	Jodhpur	0.78	NMNT	3.84**	TTS	1.42	NMPT	1.09	NMNT
19	Kharchi	1.42	NMPT	2.33*	NMNT	2.07*	NMNT	2.06*	NMPT
20	Mangaliawas	2.81**	MPT	3.22**	MPT	3.07**	NMNT	3.47**	NMNT
21	Metra City	1.45	NMNT	2.77**	NMNT	1.87	TTS	1.51	NMNT
22	Mount Abu	-1.62	TTS	-1.46	NMPT	-0.78	NMPT	-0.55	NMNT
23	Osian	2.00*	NMNT	3.15**	NMPT	2.60**	NMNT	2.58**	MPT
24	Pachpadra	4.92**	NMNT	5.17**	NMNT	7.10**	NMPT	11.74**	NMNT
25	Pali	1.54	NMPT	2.70**	NMNT	2.01*	NMNT	2.14*	MPT
26	Parbatar	0.74	NMNT	0.38	NMNT	0.28	NMNT	0.44	NMNT
27	Phalodi	0.15	NMPT	-0.24	MNT	-0.45	MNT	-0.64	MNT
28	Pindwara	1.55	NMNT	1.99*	NMNT	1.12	MPT	1.84	MPT
29	Pisangan	2.36*	TTS	3.31**	TTS	3.36**	TTS	3.27**	MPT
30	Pushkar	2.81**	MPT	4.34**	NMPT	3.42**	MPT	3.14**	MPT
31	Raipur	2.29*	MPT	3.96**	MPT	3.85**	NMPT	3.48**	MPT
32	Sanchore	0.69	TTS	1.02	MPT	3.03**	MPT	3.82**	NMNT
33	Sheo	2.01*	NMNT	2.84**	NMNT	2.76**	NMNT	2.68**	MPT
34	Sheoganj	-0.80	TTS	-3.40	TTS	-1.77	TTS	-1.45	MNT
35	Shergarh	0.56	NMNT	-0.23	NMNT	-0.93	NMNT	-0.95	NMNT
36	Sirohi	0.42	TTS	0.27	TTS	-0.06	TTS	0.22	TTS
37	Siwana	1.61	NMNT	3.75**	MPT	2.69**	MPT	3.26**	MPT
38	Sojat	1.78	NMPT	4.66**	NMPT	3.85**	NMPT	3.20**	MPT
39	Tatgarh	1.61	MPT	2.54*	MPT	1.83	MPT	2.12*	TTS

*95% confidence level, **99% confidence level, *MNT*, monotonic negative trend; *NMPT*, non-monotonic positive trend; *NMNT*, non-monotonic negative trend

Pindwara, Desuri, Phalodi, Dengana, Ajmer, Shergarh, and Mangliawas showed decreasing drought trends, and there were very few of the stations, such as Ahore, Chohtan, Sojat, and Raipur which depicted increasing trends at SPI 12-time scale by Sen’s Innovative trend (ITA, SPI 12) analysis.

However, there were only three stations that had a significant increasing trend; these are the Kharchi, Pali, and Bhinai,

and most of the stations, Mount Abu, Bilara, Ajmer, Jawaja, Jaitaran, Sirohi, Sanchore, and Parbatar, experienced the decreasing trends at SPI 24 time scale (Fig. 12), considering the 95% significant level. In addition, at the same time scale, 41% of the recorded rain gauge station among the total recorded rain gauge stations experienced monotonic positive trends. In comparison, only 10% of stations have shown

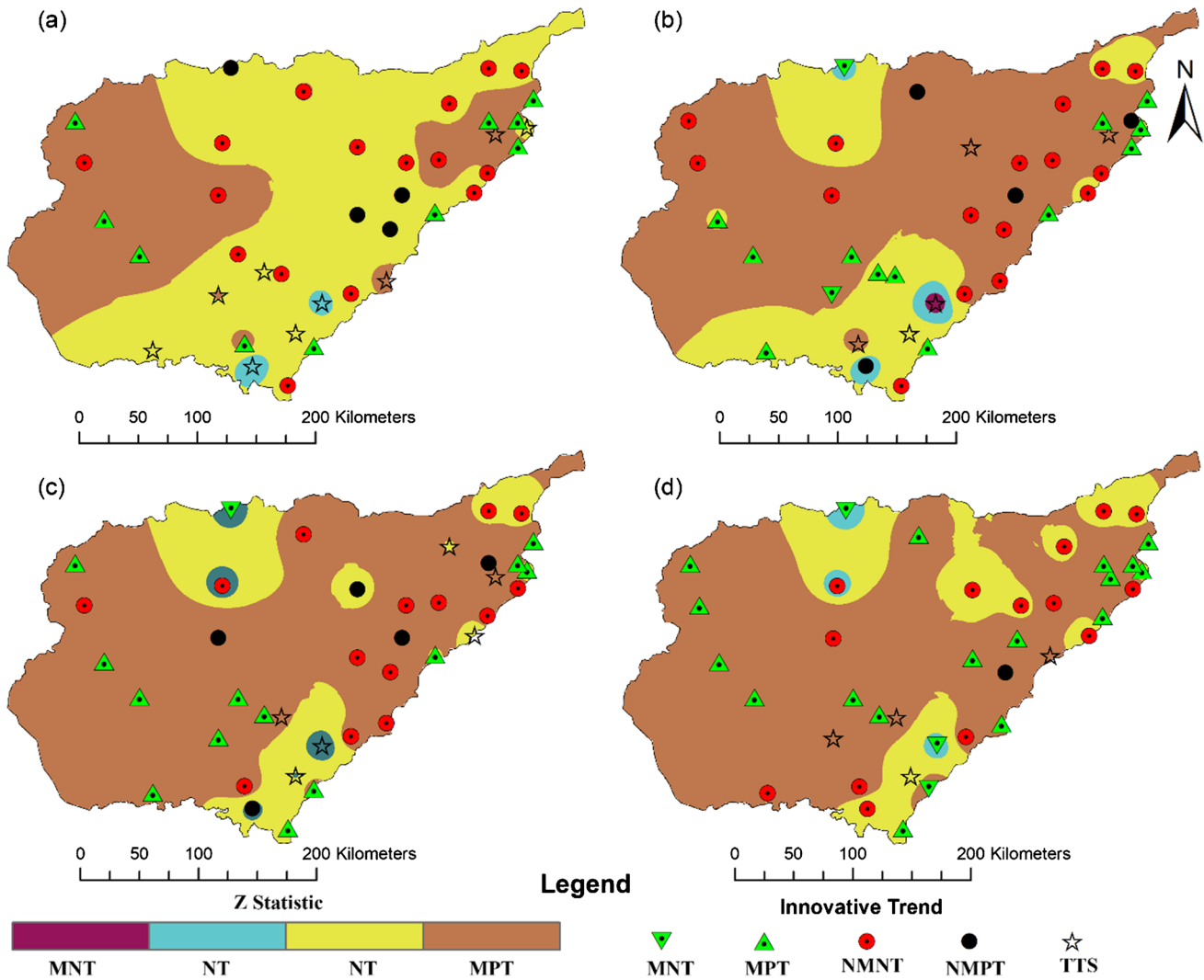


Fig. 8 Spatial patterns of drought trends **a** SPI 3, **b** SPI 6, **c** SPI 12, and **d** SPI 24

monotonic negative trends in the central, western and-eastern-part of the Luni basin area, Rajasthan (Fig. 8). There were 36% of stations identified non-monotonic negative trends. Only one station, Kharchi, revealed the non-monotonic positive trends (Table 5). Alternatively, the lengthier period of SPI 24 revealed that repeated droughts (44 to 59%) were seen in roughly 66.91% of the basin area, with these areas primarily located in the basin’s northern, eastern, and southern regions. The ITA slope distribution pattern and Z statistics results demonstrated that substantial growing trends are largely concentrated in the Luni Basin’s middle, eastern, and western regions, Rajasthan.

Discussion

In a changing climate, trend analysis of droughts with geographical and temporal variability is critical for assessing climate-induced changes and suggesting the management of hydrological scarcity for the future. The research area looks at trends in annual, seasonal, and intra-seasonal time frames. The findings of this investigation were compared with the obtained results using the MK, mMK, and ITA tests. The ITA method is more accurate and does not need any assumptions also; it avoids the necessity

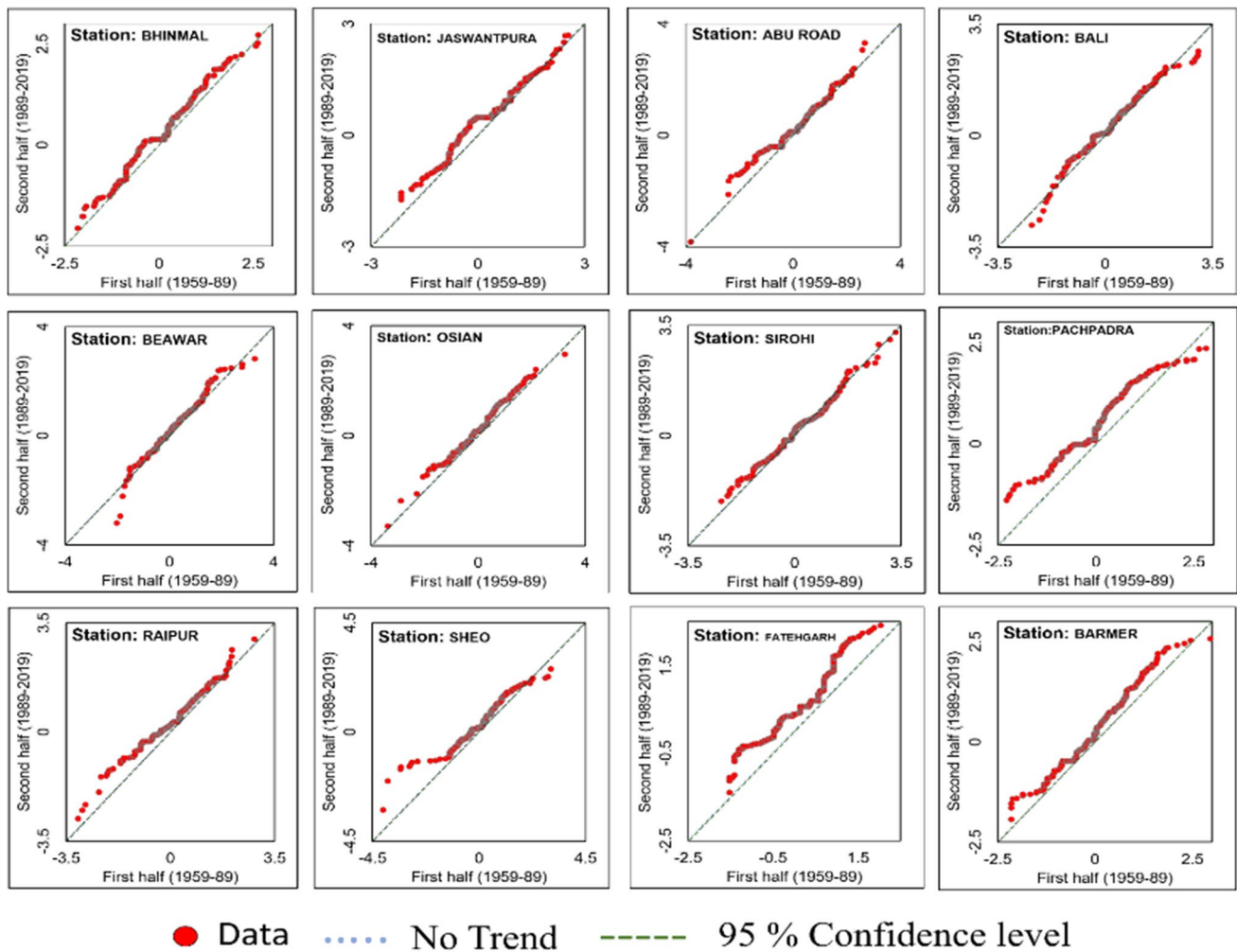


Fig. 9 Plot of SPI 3 Innovative trend analysis (ITA)

for an independent analysis step since it is based on the ascending order of the halves time series. Where Mann-Kendall trend test is dependent on assumptions and when the autocorrelation exists in natural hydro-climatological time series, that may or may not be valid. The ITA trend analysis approach has only recently been developed; thus, we utilized the Mann-Kendall test to verify its legitimacy. SPI given by McKee et al. (1993) is used mainly in data scarcity regions although it is recommended by WMO in Lincoln's declaration on drought indices (universal meteorological drought index recommended in Bulletin of the American Meteorological Society) (Hayes et al. 2011). The novelty of the study relied on this ITA analysis, which was first time tested over the study area and revealed that in the center, eastern, and western areas of the basin, substantial growing tendencies are concentrated.

There are several merits to utilizing the SPI index (Zeybekoğlu and Aktürk 2021; Rostamian et al. 2013), viz., (i) even when other hydro-meteorological variables are not

present, the SPI can still be estimated using just a single meteorological indicator (rainfall), (ii) the SPI is applicable over several time-frames, (iii) compared to the PDSI indicator, the SPI helps identify moisture deficiencies relatively quickly, and (iv) comparing to certain other measures, the SPI is a straightforward and flexible measure. In LRB of Rajasthan, climatic parameters are not available; therefore, this research is unable to compute other indices, i.e., standardized precipitation evapotranspiration index (SPEI), crop moisture index (CMI), palmer drought severity index (PDSI), drought reconnaissance index (DRI).

The difference between the previous study of Das et al. (2020a, b) with the present study on the LRB is basically manifesting the used methodological variations. Das et al. (2020a, b) employed the trend analysis with only the non-parametric MK test, but in this research, MK, mMK, and ITA methods are utilized. As the MK and mMK test can not determine the sub-trend of spatio-temporal variability of a meteorological drought event, therefore, this research

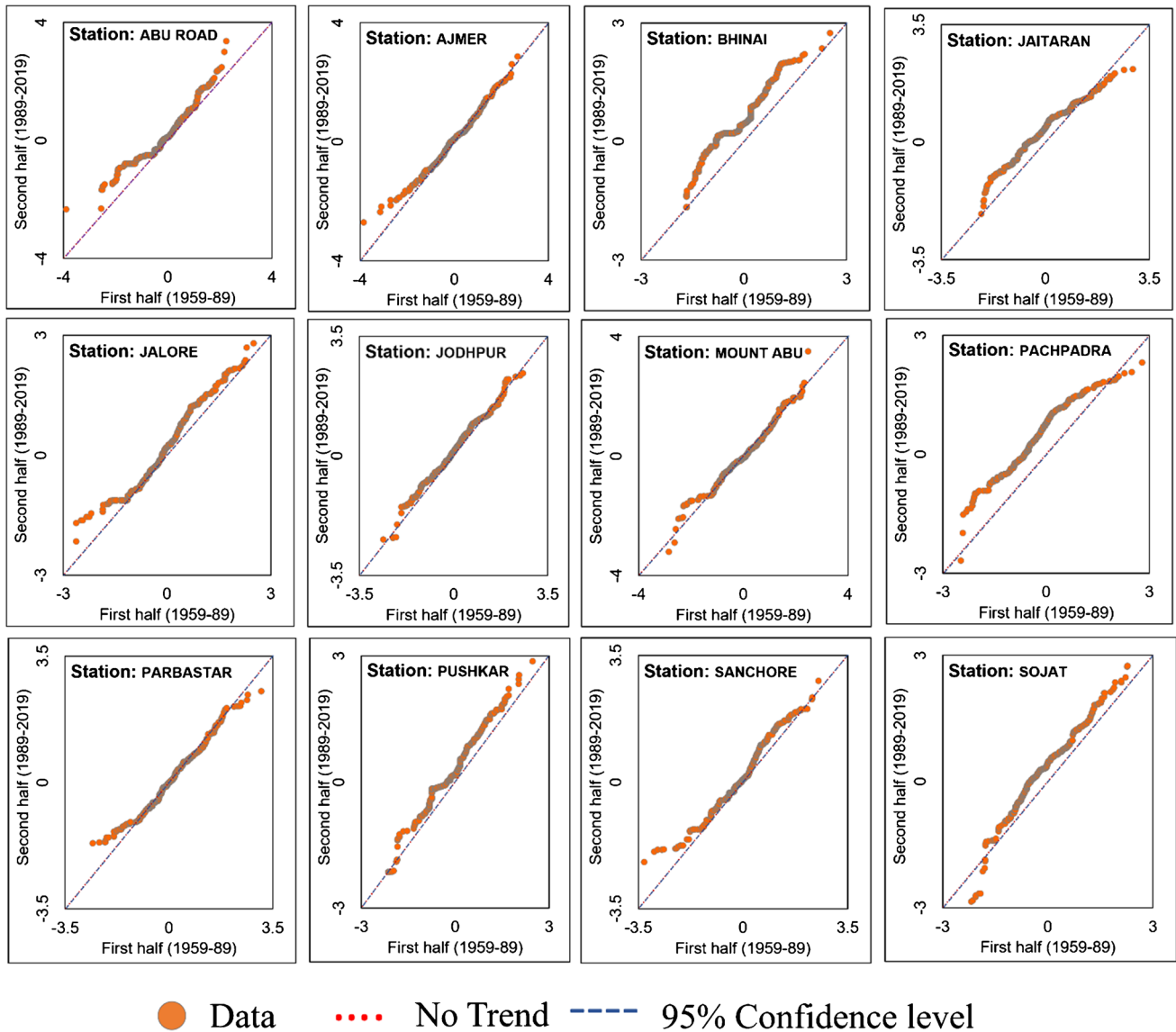


Fig. 10 Plot of SPI 6 Innovative trend analysis (ITA)

includes the ITA for analyzing the sub-trends. Besides these, the research also classifies the drought characteristics and finds the impact of IOD and ENSO in the LRB. From the observation, it is clear that the IOD has a great impact on SPI compared to ENSO as the study found the most positive correlation between IOD and SPI. The comparison of short-term SPI (SPI 3 and SPI 6) and long-term SPI (SPI 3 and SPI 6) has been also included in this investigation. The research manifests that the highest frequency of extreme drought occurrences has been found in the long-term SPI category. Therefore, mitigation measures are to be needed for implementation to reduce the impact of long-term SPI. Parallely, in the stations with increasing trends of drought frequencies, there is a need to apply sustainable water resource management techniques due to the problem of increasing water

scarcity in vulnerable places (Das et al. 2020c; Al-Maktoumi et al. 2021).

Conclusions

Many of India’s socio-economically depressed and drought-prone areas lack drought detection and evaluation for proper administration techniques and strategy formulation. However, researchers have varied viewpoints on drought assessment due to the difficulty of drought identification. This research employed SPI, MK, mMK, and ITA methods with the integration of GIS techniques to investigate monotonic and non-monotonic types of drought trends and identify the drought years and frequencies over the Luni basin for

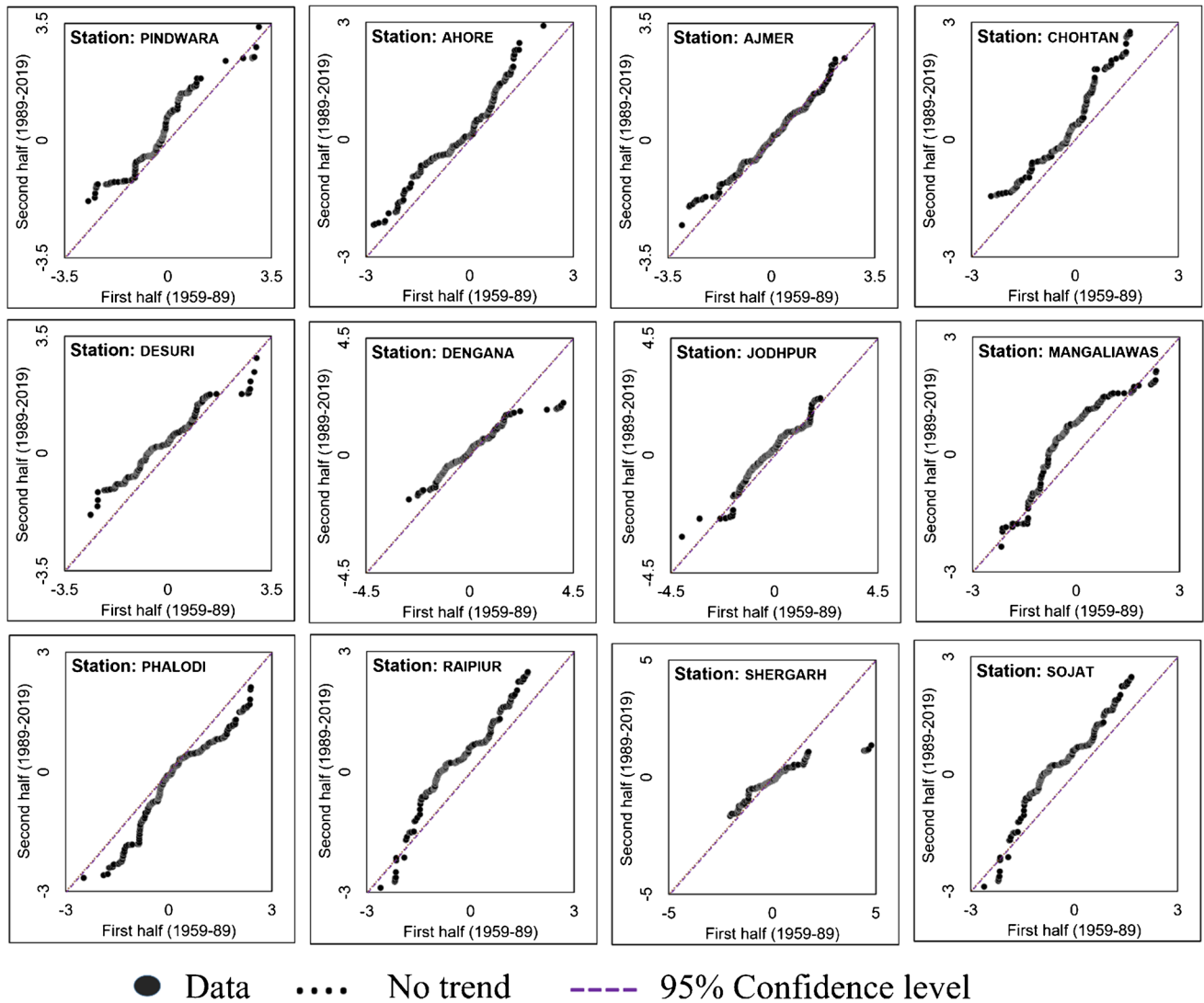
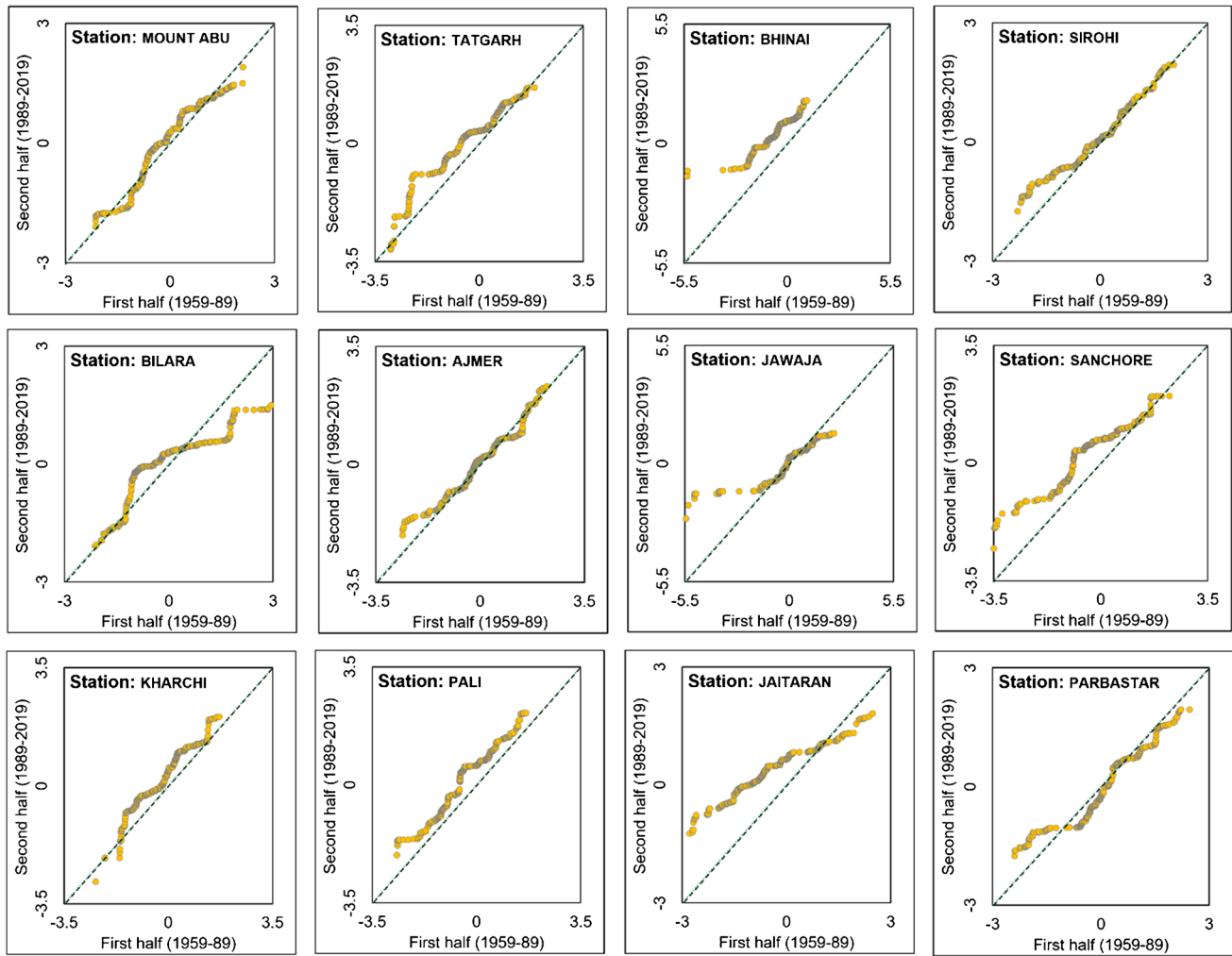


Fig. 11 SPI 12 Innovative trend analysis (ITA)

the period of 1959–2019. The different SPI timelines show distinct drought episodes and associated severity, which is highly important in the understanding of seasonal drought. By examining the rainfall trend, it was possible to conclude that the ITA result visualizes the hidden or sub-trend trend for the 39 stations, and the Z statistic supported this assertion.

The drought index in this study is constructed using the station-based time series (1959–2019) meteorological data collected across the Luni basin. These data were used to produce drought trend pattern maps for this region. This study presents a technical graph that was proposed by Şen (2012) using temporal rainfall data to detect the hidden drought trend over the Luni Basin. The result of this study depicts that more than 70% of the recorded rain gauge stations experienced two types of drought trends; these are monotonic positive trends and non-monotonic negative

trends, while 13% of the stations recorded non-monotonic negative trends. The ITA slope distribution pattern and Z statistics result demonstrated that substantial growing trends are largely concentrated in the middle, eastern, and western regions of the Luni basin, Rajasthan. The ITA trend detected 43% of the recorded rain gauge stations are experiencing a non-monotonic negative trend, and more than 23% of the recorded rain gauge stations are experiencing a monotonic positive trend, whereas only 10% show a non-monotonic positive trend. The ITA method is one that can detect patterns in different sets of data, which provides insight into extreme values. This method is also sensitive to detecting hidden trends. Non-monotonic and monotonic trend types can be determined and visualized using the innovative trend analysis (ITA) approach (Şen, 2012). The new illustration graph has given a valuable and beneficial addition to the Sen-ITA strategy for obtaining more facts about trends.



● Data ···· No Trend - - - - 95% Confidence level

Fig. 12 SPI 24 Innovative trend analysis (ITA)

This study confirmed that Sen’s newly developed technique (ITA) has been able to detect the non-monotonic trend. The obtained results from this study are crucial for creating drought coping strategies and developing future effective management plans to reduce drought impact over the study area. The major limitation of the study is that the investigation is only based on a drought index, viz., SPI. Due to lacking freely accessible meteorological data, it is not possible to compute the other indices, viz., SPEI, CMI, PDSI, and DRI. The comparison of the outcome from different drought indices is not possible for the present study which demonstrates the limitation of the research. The study can further be improved by integrating the other drought indices to determine the effective drivers of drought occurrences. To comprehend the effects of climatic variables on drought episodes, forthcoming drought forecasting experiments with

a wide number of meteorological factors should indeed be carried out.

Supplementary Information The online version contains supplementary material available at <https://doi.org/10.1007/s12517-023-11290-8>.

Declarations

Competing interests The authors declare no competing interests.

References

Achour K, Meddi M, Zeroual A, Bouabdelli S, Maccioni P, Moramarco T, Moramarco T (2020) Spatio-temporal analysis and forecasting of drought in the plains of northwestern Algeria

- using the standardized precipitation index. *J Earth Syst Sci* 129(1):1–22. <https://doi.org/10.1080/02508060.2018.1541583>
- Ahmad I, Zhang F, Tayyab M, Anjum MN, Zaman M, Liu J, Farid HU, Saddique Q (2018) Spatiotemporal analysis of precipitation variability in annual, seasonal and extreme values over upper Indus River basin. *Atmos Res*. 213:346–60. <https://doi.org/10.1016/j.atmosres.2018.06.019>
- Akturk G, Zeybekoglu U, Yildiz O (2022) Assessment of meteorological drought analysis in the Kizilirmak River Basin, Turkey. *Arab J Geosci* 15(9):1–15
- Al-Maktoumi A, Abdalla O, Kacimov A, Zekri S, Chen M, Al-Hosni T, Madani K (eds) (2021) *Water resources in arid lands: management and sustainability*. Springer International Publishing. <https://doi.org/10.1007/978-3-030-67028-3>
- Alsubih M, Mallick J, Talukdar S, Salam R, AlQadhi S, Fattah MA, Thanh NV (2021) An investigation of the short-term meteorological drought variability over Asir Region of Saudi Arabia. *Theor Appl Climatol* 13:1–21. <https://doi.org/10.1007/s00704-021-03647-4>
- Basak A, Das J, Rahman ATMS, Pham QB (2021) An integrated approach for delineating and characterizing groundwater depletion hotspots in a coastal state of India. *J Geol Soc India* 97(11):1429–1440. <https://doi.org/10.1007/s12594-021-1883-z>
- Basak A, Rahman AS, Das J, Hosono T, Kisi O (2022) Drought forecasting using the Prophet model in a semi-arid climate region of western India. *Hydrol Sci J* 67:1397–1417. <https://doi.org/10.1080/02626667.2022.2082876>
- Benzater B, Elouissi A, Dabanli I, Benaricha B, Hamimed A (2021) Extreme rain trend analysis in Macta watershed North West Algeria. *Arab J Geosci* 14(4):1–4. <https://doi.org/10.1007/s12517-021-06636-z>
- Buttafuoco G, Caloiero T, Coscarelli R (2015) Analyses of drought events in Calabria (Southern Italy) using standardized precipitation index. *Water Resour Manag*. 29(2):557–73. <https://doi.org/10.1007/s11269-014-0842-5>
- Caloiero T (2020) Evaluation of rainfall trends in the South Island of New Zealand through the innovative trend analysis (ITA). *Theor Appl Climatol* 139(1):493–504. <https://doi.org/10.1007/s00704-019-02988-5>
- Chhajjer D, Naidu K, Shah NV (2015) Study of impact of celebrity endorsement on consumer buying behaviour. *International Conference on Technology and Business Management*. pp 417–423
- Citakoglu H, Coşkun Ö (2022) Comparison of hybrid machine learning methods for the prediction of short-term meteorological droughts of Sakarya Meteorological Station in Turkey. *Environ Sci Pollut Res* 1–25.
- Czerniak A, Grajewski S, Krysztofiak-Kaniewska A, Kurowska EE, Okoński B, Górna M, Borkowski R (2020) Engineering methods of forest environment protection against meteorological drought in Poland. *Forests* 11(6):614. <https://doi.org/10.3390/f11060614>
- Dabanlı İ, Mishra AK, Şen Z (2017) Long-term spatio-temporal drought variability in Turkey. *J Hydrol*. 552:779–92. <https://doi.org/10.1016/j.jhydrol.2017.07.038>
- Das J (2012) Probability and variability analysis of rainfall characteristics of Dinhat in Koch Behar district of West Bengal. *Golden Research Thoughts* 2(1):1–9
- Das J, Bhattacharya SK (2018) Trend analysis of long-term climatic parameters in Dinhat of Koch Bihar district, West Bengal. *Spat Inf Res* 26(3):271–280. <https://doi.org/10.1007/s41324-018-0173-3>
- Das J, Mandal T, Saha P (2019) Spatio-temporal trend and change point detection of winter temperature of North Bengal, India. *Spat Inf Res*. 27(4):411–24. <https://doi.org/10.1007/s41324-019-00241-9>
- Das J, Gayen A, Saha P, Bhattacharya SK (2020a) Meteorological drought analysis using standardized precipitation index over Luni River Basin in Rajasthan, India. *SN Appl Sci*. 2(9):1–7. <https://doi.org/10.1007/s42452-020-03321-w>
- Das J, Mandal T, Sahab P, Kumar Bhattacharya S (2020b) Variability and trends of rainfall using non-parametric approaches: a case study of semi-arid area. *Mausam*. 71(1):33–44
- Das J, Rahman AS, Mandal T, Saha P (2020c) Challenges of sustainable groundwater management for large scale irrigation under changing climate in Lower Ganga River basin in India. *Groundwater Sustain Dev* 11:100449. <https://doi.org/10.1016/j.gsd.2020.100449>
- Das J, Sakiur RATM, Tapash M, Piu S (2021a) Exploring driving forces of large-scale unsustainable groundwater development for irrigation in lower Ganga River basin in India. *Environ Dev Sustain* 23(5):7289–7309. <https://doi.org/10.1007/s10668-020-00917-5>
- Das J, Mandal T, Rahman ATM, Saha P (2021b) Spatio-temporal characterization of rainfall in Bangladesh: an innovative trend and discrete wavelet transformation approaches. *Theor Appl Climatol* 143(3):1557–1579
- de Brito CS, da Silva RM, Santos CA, Neto RM, Coelho VH (2021) Monitoring meteorological drought in a semi-arid region using two long-term satellite-estimated rainfall datasets: a case study of the Piranhas River basin, northeastern Brazil. *Atmos Res*. 250:105380. <https://doi.org/10.1016/j.atmosres.2020.105380>
- Dehghani M, Saghafian B, Nasiri Saleh F, Farokhnia A, Noori R (2014) Uncertainty analysis of streamflow drought forecast using artificial neural networks and Monte-Carlo simulation. *Int J Climatol*. 34(4):1169–80. <https://doi.org/10.1002/joc.3754>
- Demir V (2022) Trend analysis of lakes and sinkholes in the Konya Closed Basin, in Turkey. *Nat Hazards*. <https://doi.org/10.1007/s11069-022-05327-6>
- Demir V, Keskin AÜ (2020) Water level change of lakes and sinkholes in Central Turkey under anthropogenic effects. *Theor Appl Climatol* 142:929–943. <https://doi.org/10.1007/s00704-020-03347-5>
- Edwards DC (1997) Characteristics of 20th Century drought in the United States at multiple time scales. *Air Force Inst of Tech Wright-Patterson Afb Oh*
- Ganguli P, Reddy MJ (2013) Analysis of ENSO-based climate variability in modulating drought risks over western Rajasthan in India. *J Earth Syst Sci*. 122(1):253–69
- Ganguli P, Reddy MJ (2014) Ensemble prediction of regional droughts using climate inputs and the SVM–copula approach. *Hydrol Process*. 28(19):4989–5009. <https://doi.org/10.1002/hyp.9966>
- Golian S, Mazdiyasnı O, AghaKouchak A (2015) Trends in meteorological and agricultural droughts in Iran. *Theor Appl Climatol*. 119(3):679–88. <https://doi.org/10.1007/s00704-014-1139-6>
- Gupta A, Dimri AP, Thayyen R, Jain S, Jain S (2020) Meteorological trends over Satluj River Basin in Indian Himalaya under climate change scenarios. *J Earth Syst Sci*. 129(1):1–8. <https://doi.org/10.1007/s12040-020-01424-x>
- Gupta P, Tignath S, Kathal D, Choudhury S, Mukherjee K, Das J, Das J, Bhattacharya SK (2023) Monitoring and managing multi-hazards a multidisciplinary approach groundwater depletion zonation using geospatial technique and TOPSIS in Raipur District Chhattisgarh India. *Springer International Publishing Cham*, pp 237–7251
- Haktanir T, Citakoglu H (2015) Closure to “Trend, independence, stationarity, and homogeneity tests on maximum rainfall series of standard durations recorded in Turkey” by Tefaruk Haktanir and Hatice Citakoglu. *J Hydrol Eng* 20(10):07015017
- Hayes M, Svoboda M, Wall N, Widhalm M (2011) The Lincoln declaration on drought indices: universal meteorological drought index recommended. *Bull Am Meteorol Soc* 92(4):485–488. <https://doi.org/10.1175/2010BAMS3103.1>
- Hlanze DK, Mulungu DMM, Ndomba P, Tfwala S, Mabaso S, Dlamini WM, Gumindoga W, Mitra R, Das J (2023) Estimating soil loss rate and sediment yield of the proposed Ngololweni Earth

- Dam, Kingdom of Eswatini. Monitoring and Managing Multi-hazards. Springer, Cham, pp 33–64. https://doi.org/10.1007/978-3-031-15377-8_3
- Kamruzzaman M, Rahman ATMS, Basak A, Alam J, Das J (2022) Assessment and adaptation strategies of climate change through the prism of farmers' perception: A case study. *Int J Environ Sci Technol*. <https://doi.org/10.1007/s13762-022-04254-0>
- Kendall MG (1975) *Multivariate analysis*. Griffin, London
- Khera R (2006) Political economy of state response to drought in Rajasthan, 2000–03. *Econ Polit Wkly*. 16:5163–72
- Kumar V, Jain SK (2011) Trends in rainfall amount and number of rainy days in river basins of India (1951–2004). *Hydrol Res*. 42(4):290–306. <https://doi.org/10.2166/nh.2011.067>
- Kuriqi A, Ali R, Pham QB, Gambini JM, Gupta V, Malik A, Linh NT, Joshi Y, Anh DT, Dong X (2020) Seasonality shift and stream-flow variability trends in central India. *Acta Geophys*. 68(5):1461–75. <https://doi.org/10.1007/s11600-020-00475-4>
- Mall RK, Singh R, Gupta A, Srinivasan G, Rathore LS (2006) Impact of climate change on Indian agriculture: a review. *Clim Change*. 78(2):445–478. <https://doi.org/10.1007/s10584-006-9236-x>
- Mallick J, Talukdar S, Alsubih M, Salam R, Ahmed M, Kahla NB, Shamimuzzaman M (2021) Analysing the trend of rainfall in Asir region of Saudi Arabia using the family of Mann-Kendall tests, innovative trend analysis, and detrended fluctuation analysis. *Theor Appl Climatol*. 143(1):823–41. <https://doi.org/10.1007/s00704-020-03448-1>
- Mandal T, Das J, Rahman ATMS, Saha P, Haldar RA, Alam A, Satpati L (2021a) Habitat Ecology and Ekistics Case Studies of Human-Environment Interactions in India Rainfall Insight in Bangladesh and India: Climate Change and Environmental Perspective. Springer International Publishing Cham, pp 53–74
- Mandal T, Sarkar A, Das J, Rahman ATMS, Chouhan P, Islam MN, van Amstel A (2021b) India: Climate Change Impacts Mitigation and Adaptation in Developing Countries Comparison of Classical Mann-Kendall Test and Graphical Innovative Trend Analysis for Analyzing Rainfall Changes in India. Springer International Publishing Cham, pp 155–183
- Mandal T, Saha S, Das J, Sarkar A (2022) Groundwater depletion susceptibility zonation using TOPSIS model in Bhagirathi river basin, India. *Model Earth Syst Environ* 8(2):1711–1731. <https://doi.org/10.1007/s40808-021-01176-7>
- Mann HB (1945) Non-parametric tests against trend. *Econom J Econom Soc*. 1:245–59
- Masroor M, Rehman S, Avtar R, Sahana M, Ahmed R, Sajjad H (2020) Exploring climate variability and its impact on drought occurrence: evidence from Godavari Middle sub-basin, India. *Weather Clim Extrem*. 30:100277. <https://doi.org/10.1016/j.wace.2020.100277>
- McKee TB, Doesken NJ, Kleist J (1993) The relationship of drought frequency and duration to time scales. *Proc 8th Conf Appl Climatol*. 17(22):179–183
- Mishra V, Thirumalai K, Jain S, Aadhar S (2021) Unprecedented drought in South India and recent water scarcity. *Environ Res Lett*. 16(5):054007
- Mitra R, Das J (2022) A comparative assessment of flood susceptibility modelling of GIS-based TOPSIS, VIKOR, and EDAS techniques in the Sub-Himalayan foothills region of Eastern India. *Environ Sci Pollut Res*. <https://doi.org/10.1007/s11356-022-23168-5>
- Mitra R, Kumar Mandal D (2022) Assessment of livelihood vulnerability in the riparian region of the Tista River, West Bengal, India. *Geo J* 1-29. <https://doi.org/10.1007/s10708-022-10645-0>
- Mitra R, Saha P, Das J (2022) Assessment of the performance of GIS-based analytical hierarchical process (AHP) approach for flood modelling in Uttar Dinajpur district of West Bengal, India. *Geomatics Nat Hazards Risk* 13(1):2183–2226. <https://doi.org/10.1080/19475705.2022.2112094>
- Mitra R, Roy D (2022) Delineation of groundwater potential zones through the integration of remote sensing, geographic information system, and multi-criteria decision-making technique in the sub-Himalayan foothills region, India. *Int J Energy Water Res* 1-21. <https://doi.org/10.1007/s42108-022-00181-5>
- Mundetia N, Sharma D (2015) Analysis of rainfall and drought in Rajasthan State, India. *Global Nest*. 17(1):12–21
- Murthy CS, Sessa Sai MV (2010) Agriculture drought monitoring and assessment. *remote Sensing*
- Patel NR, Chopra P, Dadhwal VK (2007) Analyzing spatial patterns of meteorological drought using standardized precipitation index. *Meteorol Appl J Forecast Pract Appl Train Tech Model*. 14(4):329–36. <https://doi.org/10.1002/met.33>
- Pathak AA, Dodamani BM (2020) Trend analysis of rainfall, rainy days and drought: a case study of Ghataprabha River Basin, India. *Model Earth Syst Environ*. 6(3):1357–72. <https://doi.org/10.1007/s40808-020-00798-7>
- Piniowski M, Marcinkowski P, Kundzewicz ZW (2018) Trend detection in river flow indices in Poland. *Acta Geophys*. 66(3):347–60. <https://doi.org/10.1007/s11600-018-0116-3>
- Poddar I, Alam J, Basak A, Mitra R, Das J (2023) Application of a geospatial-based subjective MCDM method for flood susceptibility modeling in Teesta River Basin, West Bengal, India. *Monitoring and Managing Multi-hazards*. Springer, Cham, pp 135–152. https://doi.org/10.1007/978-3-031-15377-8_10
- Rathore JS (2004) Drought and household coping strategies: a case of Rajasthan. *Indian J Agric Econ*. 59(4):689–708
- Rostamian R, Eslamian S, Farzaneh MR (2013) Application of standardised precipitation index for predicting meteorological drought intensity in Beheshtabad watershed, central Iran. *Int J Hydrol Sci Technol* 3(1):63–77
- Roy D, Das S, Mitra R (2022) An application of geospatial-based multi-criteria decision-making technique to identify landslide susceptibility zones in the Ragnu Khola River Basin of Darjeeling Himalayan region India. *Appl Geomat* 14(4):731–749. <https://doi.org/10.1007/s12518-022-00468-6>
- Saha P, Mitra R, Chakraborty K, Roy M (2022) Application of multi layer perceptron neural network Markov Chain model for LULC change detection in the Sub-Himalayan North Bengal. *Remote Sens Appl Soc Environ* 26:100730. <https://doi.org/10.1016/j.rsase.2022.100730>
- Şen Z (2012) Innovative trend analysis methodology. *J Hydrol Eng*. 17(9):1042–6. [https://doi.org/10.1061/\(ASCE\)HE.1943-5584.0000556](https://doi.org/10.1061/(ASCE)HE.1943-5584.0000556)
- Shewale MP, Kumar S (2005) Climatological features of drought incidences in India. *Meteorological Monograph (Climatology 21/2005)*. National Climate Centre, Indian Meteorological Department
- Sirdaş S, Sen Z (2003) Spatio-temporal drought analysis in the Trakya region, Turkey. *Hydrol Sci J*. 48(5):809–20. <https://doi.org/10.1623/hysj.48.5.809.51458>
- Thom HC (1958) A note on the gamma distribution. *Mon Weather Rev*. 86(4):117–122. [https://doi.org/10.1175/1520-0493\(1958\)086%3C0117:ANOTGD%3E2.0.CO;2](https://doi.org/10.1175/1520-0493(1958)086%3C0117:ANOTGD%3E2.0.CO;2)
- Tran TV, Tran DX, Huynh PD, Dao HN, Vo TM, Trinh HP, Tran XQ (2020) Analysing drought intensity in the Mekong River Delta using time series analysis and Google Earth Engine. *Int J Geoinformatics* 16(1).
- Uddin MJ, Hu J, Islam AR, Eibek KU, Nasrin ZM (2020) A comprehensive statistical assessment of drought indices to monitor drought status in Bangladesh. *Arab J Geosci*. 13(9):1. <https://doi.org/10.1007/s12517-020-05302-0>
- Yagbasan O, Yazicigil H, Demir V (2017) Impacts of climatic variables on water-level variations in two shallow Eastern Mediterranean lakes. *Environ Earth Sci* 76:575. <https://doi.org/10.1007/s12665-017-6917-x>

- Yin Y, Xu CY, Chen H, Li L, Xu H, Li H, Jain SK (2016) Trend and concentration characteristics of precipitation and related climatic teleconnections from 1982 to 2010 in the Beas River basin, India. *Glob Planet Change*. 145:116–29. <https://doi.org/10.1016/j.gloplacha.2016.08.011>
- Yue S, Wang C (2004) The Mann-Kendall test modified by effective sample size to detect trend in serially correlated hydrological series. *Water Res Manag*. 18(3):201–18. <https://doi.org/10.1023/B:WARM.0000043140.61082.60>
- Zeybekoğlu U, Aktürk G (2021) A comparison of the China-Z index (CZI) and the standardized precipitation index (SPI) for drought assessment in the Hirfanlı Dam basin in central Turkey. *Arab J Geosci* 14(24):1–13
- Zhang R, Chen ZY, Xu LJ, Ou CQ (2016) Meteorological drought forecasting based on a statistical model with machine learning techniques in Shaanxi province, China. *Sci Total Environ*. 665:338–46
- Zhao R, Wang H, Zhan C, Hu S, Ma M, Dong Y (2020) Comparative analysis of probability distributions for the standardized precipitation index and drought evolution in China during 1961–2015. *Theor Appl Climatol*. 139(3):1363–77. <https://doi.org/10.1007/s00704-019-03050-0>

Springer Nature or its licensor (e.g. a society or other partner) holds exclusive rights to this article under a publishing agreement with the author(s) or other rightsholder(s); author self-archiving of the accepted manuscript version of this article is solely governed by the terms of such publishing agreement and applicable law.